CENTRAL RESEARCH LIBRARY
DOCUMENT COLLECTION

OAK RIDGE NATIONAL LABORATORY
operated by
UNION CARBIDE CORPORATION
NUCLEAR DIVISION
for the
U.S. ATOMIC ENERGY COMMISSION

UNION CARBIDE

ORNL-TM-1613

OAK RIDGE NATIONAL LABORATORY LIBRARY
3 4456 0023725 0

61

Thermal Radiation Performance of A Finned Tube With A Reflector

R. S. Holcomb
F. E. Lynch

CENTRAL RESEARCH LIBRARY
DOCUMENT COLLECTION
LIBRARY LOAN COPY
DO NOT TRANSFER TO ANOTHER PERSON
If you wish someone else to see this document, send in name with document and the library will arrange a loan.

NOTICE This document contains information of a preliminary nature and was prepared primarily for internal use at the Oak Ridge National Laboratory. It is subject to revision or correction and therefore does not represent a final report.

LEGAL NOTICE

This report was prepared as an account of Government sponsored work. Neither the United States, nor the Commission, nor any person acting on behalf of the Commission:

A. Makes any warranty or representation, expressed or implied, with respect to the accuracy, completeness, or usefulness of the information contained in this report, or that the use of any information, apparatus, method, or process disclosed in this report may not infringe privately owned rights; or

B. Assumes any liabilities with respect to the use of, or for damages resulting from the use of any information, apparatus, method, or process disclosed in this report.

As used in the above, "person acting on behalf of the Commission" includes any employee or contractor of the Commission, or employee of such contractor, to the extent that such employee or contractor of the Commission, or employee of such contractor prepares, disseminates, or provides access to, any information pursuant to his employment or contract with the Commission, or his employment with such contractor.

ORNL-TM-1613

Contract No. W-7405-eng-26

REACTOR DIVISION

THERMAL RADIATION PERFORMANCE OF A FINNED TUBE WITH A REFLECTOR

R. S. Holcomb
F. E. Lynch

APRIL 1967

OAK RIDGE NATIONAL LABORATORY
Oak Ridge, Tennessee
operated by
UNION CARBIDE CORPORATION
for the
U.S. ATOMIC ENERGY COMMISSION

OAK RIDGE NATIONAL LABORATORY LIBRARY
3 4456 0023725 0

CONTENTS

	Page
ABSTRACT	1
INTRODUCTION	1
APPARATUS	5
Test Section	5
Vacuum and Cooling Systems	6
Electrical System	9
Instrumentation	9
PROCEDURE	12
METHOD OF CALCULATION	14
Local Heat Transfer Rates	14
Reflector Effectiveness	17
Heat Transfer Rate for a Uniform Tube Temperature	19
RESULTS AND DISCUSSION	20
Temperature Distribution on Radiator Tube and Fins	20
Variation of Heat Transfer Rate on Radiator Tube and Fins	23
Thermal Performance	23
Heat Transfer in a Vacuum	25
Heat Transfer at Atmospheric Pressure	27
Reflector and Shutter Temperature	29
Convection Heat Transfer vs Air Pressure	29
Convection Heat Transfer vs Temperature	33
Calculated Results	33
Local Heat Transfer Rates	33
Reflector Effectiveness	36
Heat-Transfer Rate for Uniform Tube Temperature	39
SUMMARY OF RESULTS	43
REFERENCES	44
APPENDIX A. METHOD OF CALCULATION OF ANGLE FACTORS	47
Tube Angle Factors	47
Fin Angle Factors	50
APPENDIX B. TABULAR RESULTS OF EXPERIMENTS	53

THERMAL RADIATION PERFORMANCE OF A FINNED TUBE WITH A REFLECTOR

R. S. Holcomb
F. E. Lynch

ABSTRACT

The thermal performance has been experimentally determined for an electrically heated, finned tube with a reflector that simulates one-half the length of a tube of the Large Potassium System radiator. The test section consisted of a 0.625-in.-OD cartridge heater rod with three fins 1.288 in. wide, made of 0.030 in. thick copper clad with 0.005 in. thick stainless steel. The heated length was 42 in.

Surface temperatures were measured for linear heat transfer rates up to 4400 Btu/hr-ft. The performance was investigated with a radiation baffle to increase the temperature at low heat loads, with the back of the reflector insulated, and at air pressures from atmospheric to 2 mm Hg absolute.

The results of the experiments are presented as graphs of linear heat-transfer rate versus fin-base temperature and as plots of the temperature distribution on the tube and fins. The linear heat-transfer rate in a vacuum could be correlated with the average fin-base temperature by the following equation:

$$q = 2.528 \times 10^{-11} T^{5.5}$$

The calculated performance of the radiator tube is presented for the ideal case of a uniform tube surface temperature.

INTRODUCTION

The experiments described in this memorandum were performed to determine the heat-transfer characteristics of a finned electric cartridge heater designed to simulate half the length of a tube of the Large Potassium System (LPS) radiator.[1] The experiments were designed to obtain the temperature distribution across the heater rod and fins as a function of the heat

generation rate with a reflecting shutter open or closed in air at pressures from atmospheric to 2 mm Hg absolute.

The LPS radiator consists of finned, tapered tubes, 7 ft in length, arranged on an 8-in. pitch in a 10-ft-diam circle. The tubes are vertical, and taper from an ID of 1.1 in. at the top to 0.3 in. at the bottom. Three fins of copper clad with stainless steel are brazed to each tube. A double-curved circular arc aluminum reflector treated by the Alzak process to give high reflectivity is attached to the center fin of each tube. A cross section of the radiator and reflector configuration is shown in Fig. 1. The tubes are welded to ring manifolds at the top and bottom to form a tube bank. Two of these tube banks compose the complete radiator for the LPS (see Fig. 2).

The circular configuration of the LPS radiator was chosen to test the performance of a near-optimum design for space power plant applications. The key features of the design are the reflectors and shutters. The reflectors serve to make the back of the tubes effective for heat removal by reflecting the heat away from the fins outward into space. This is accomplished by making the reflector of two cylindrical surfaces, each having a radius equal to the distance between the tips of adjacent fins with its center at the tip of the side fin. With a perfectly specular surface on the reflector, each ray from the radiator that strikes the reflector will be reflected at an equal and opposite angle. As shown in Fig. 1, a ray from any point on the radiator will leave the reflector in a direction such that it will not intercept the radiator surfaces.[2] The shutters can be closed to maintain higher temperatures and, consequently, higher potassium vapor pressures for part-load operation. The higher pressures are desirable to provide cavitation suppression head for the scavenging pump and to avoid excessive vapor velocities.[3,4]

The LPS radiator will give up its heat to water-cooled walls on both the inside and outside of the radiator. The inside water wall is provided to cool the reflector in case it should run hotter than anticipated. In the LPS tests the radiator enclosure was designed to be open to the atmosphere so that the radiator would also be cooled by free convection.

ORNL DWG. 67-3163

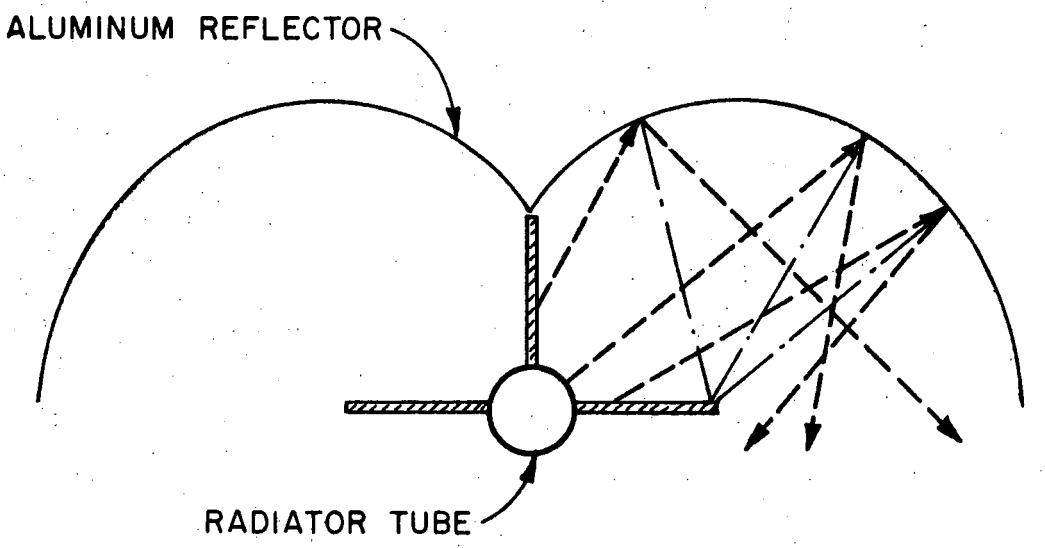

Fig. 1. Cross Section Through LPS Radiator Tube and Reflector.

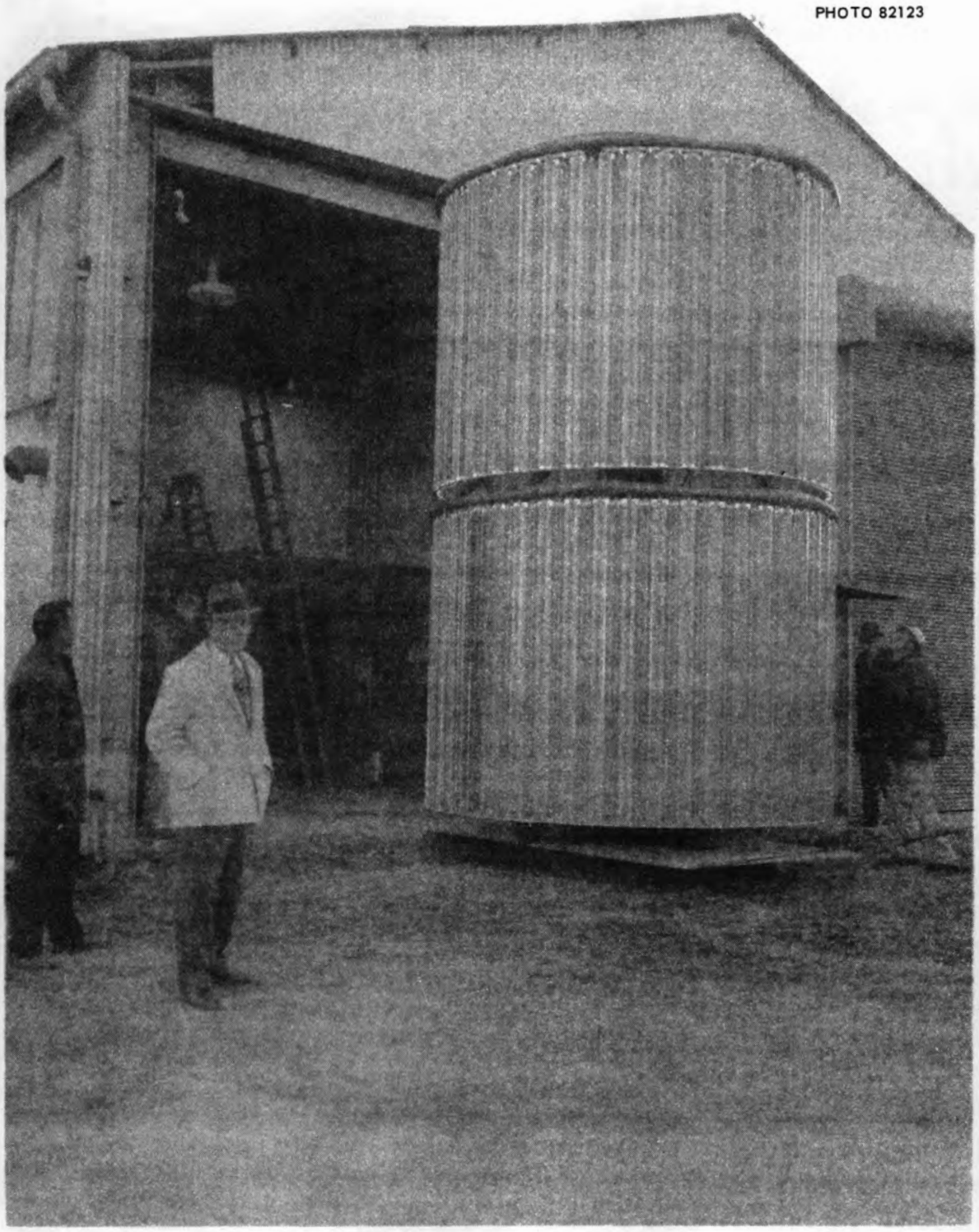

Fig. 2. Large Potassium System Radiator.

The test on the electrically heated simulated radiator tube was designed to determine its heat transfer performance for the conditions to be encountered both in the operation of the LPS and in a space environment. Surface temperatures were measured with the shutter open and closed, with and without cooling on the back of the reflector, and at air pressures from atmospheric to 2 mm Hg absolute.

APPARATUS

Test Section

The test section consisted of an electrical cartridge heater enclosed in a stainless steel tubular sheath 0.035 in. thick with an outside diameter of 0.625 in. The heater had an overall length of 54 in. with 14 heater coils along a 42-in.-long section beginning 6 in. from the end. There was a space of approximately 0.17 in. between adjacent heating coils so that the total length of the 14 coils was 39.8 in. The heater had a power rating of 5000 watts at 230 volts ac.

Three longitudinal fins were attached by brazing to the heater sheath at 0, 90, and 180 deg around the tube. The fins were made from a three-layer composite with 0.005 in. thick layer of stainless steel on both sides of an inner layer of copper 0.030 in. thick. Each fin was 1.288 in. wide and 43 in. long.

A reflector made of Alzak process aluminum with the polished surface toward the heater was fastened to the center fin at two points with stainless steel clips. The reflector was composed of two cylindrical surfaces, each extending from the tip of the center fin to a point 2.4 in. from the tip of the side fins along a diameter through the center of the heater tube. The reflector arcs had a radius of curvature of 2.4 in., because the center of curvature was designed to coincide with the tip of the side fin. The reflector was 44.5 in. long.

The surface of the finned heater and the back of the reflector were covered with a thin coat of a high emissivity ceramic silicone paint,

designated commercially as PT-404-A, which was procured from the Product Techniques Corporation. This paint increased the radiant heat-transfer capabilities, since it has a much higher emissivity than the mill finish metal.

Shutters of two designs were tested. One was made of mill finish aluminum in the shape of a semicircle with a 4-in. radius and a length of 46 in. The other was made of Alzak process polished aluminum in a flat rectangular sheet 8 in. wide and 46 in. long, with baffles to reduce convection at the ends of the reflector. The shutters were mounted on aluminum angle sections to which the edges of the reflector were attached.

The heater was mounted vertically on a lava insulator on a bottom circular plate made of aluminum. The bottom plate was hung by four 1/2-in.-diam aluminum tie rods from the lid of the vacuum tank. The heater extended through a top plate mounted on the threaded tie rods by means of eight nuts. The angle sections that supported the reflector and shutter were attached to the bottom plate and were fitted into slots in the top plate. The test section assembly with the flat shutter in the open position is shown in Fig. 3. A photograph of the curved shutter is shown in Fig. 4.

Vacuum and Cooling Systems

The test section assembly was installed in a cylindrical tank which served as a heat sink and a vacuum enclosure. The tank was fabricated from 1/4-in.-thick carbon steel plate, rolled into a cylinder with an inside diameter of 16 in. and a length of 61 in. The bottom of the tank was sealed with a 1/2-in.-thick plate, welded to the tank. A 3/4-in.-thick flange with twelve 5/8-in.-diam bolt holes was welded to the top of the tank. A cooling water annulus was formed by welding 1/8-in.-thick carbon steel sheet to two longitudinal strips of 1/8 in. x 1 in. bar stock on the outside of the tank. The inside of the tank was coated with PT-404-A high emissivity paint. The tank lid was made from 1/2-in.-thick plate. It was bolted to the flange and was sealed with a flat rubber gasket.

Cooling water was supplied to the bottom of the annulus through two manifolds made of 3/4-in. copper tubing, each of which had five branches, 30 deg apart, connected to the annulus by silver solder. Manifolds

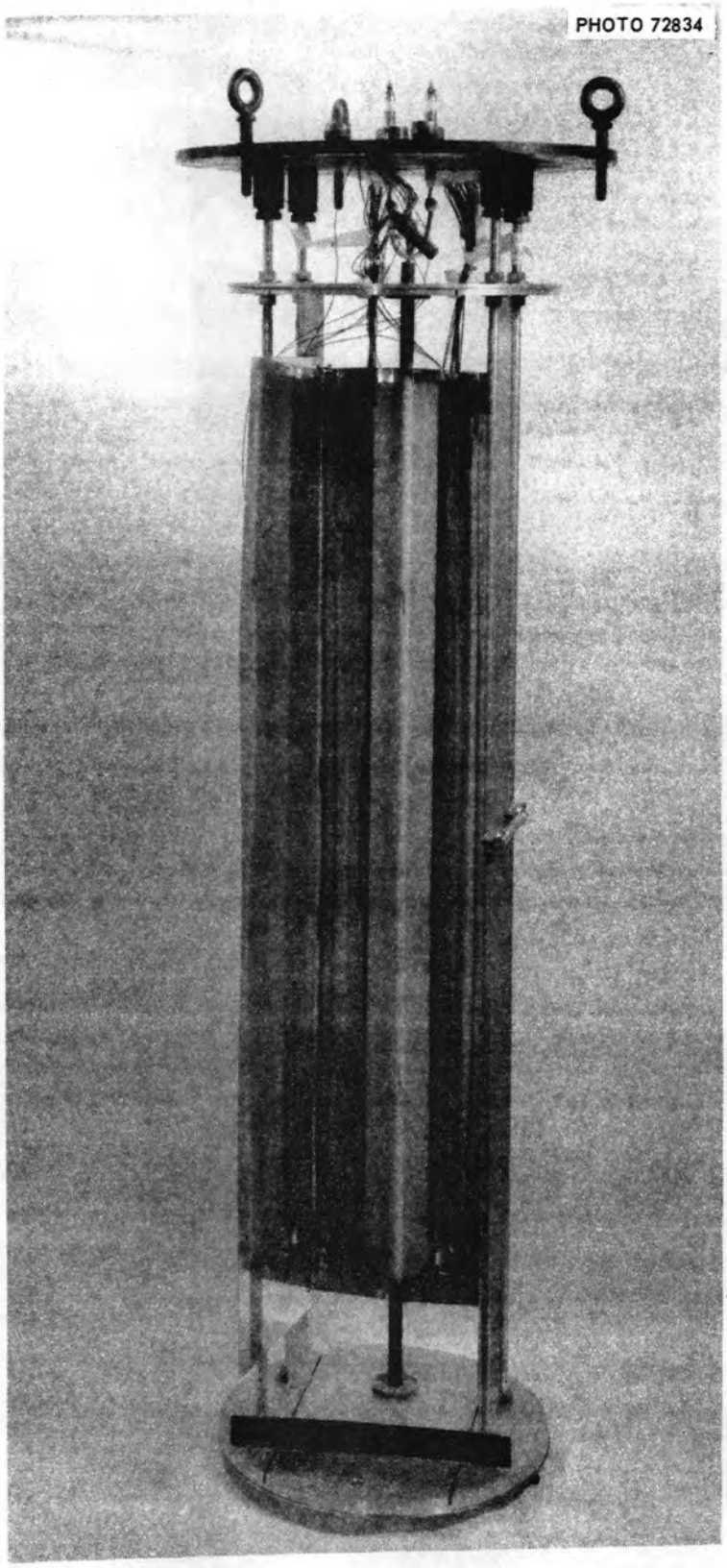

Fig. 3. Test Section Assembly with the Flat Shutter in the Open Position.

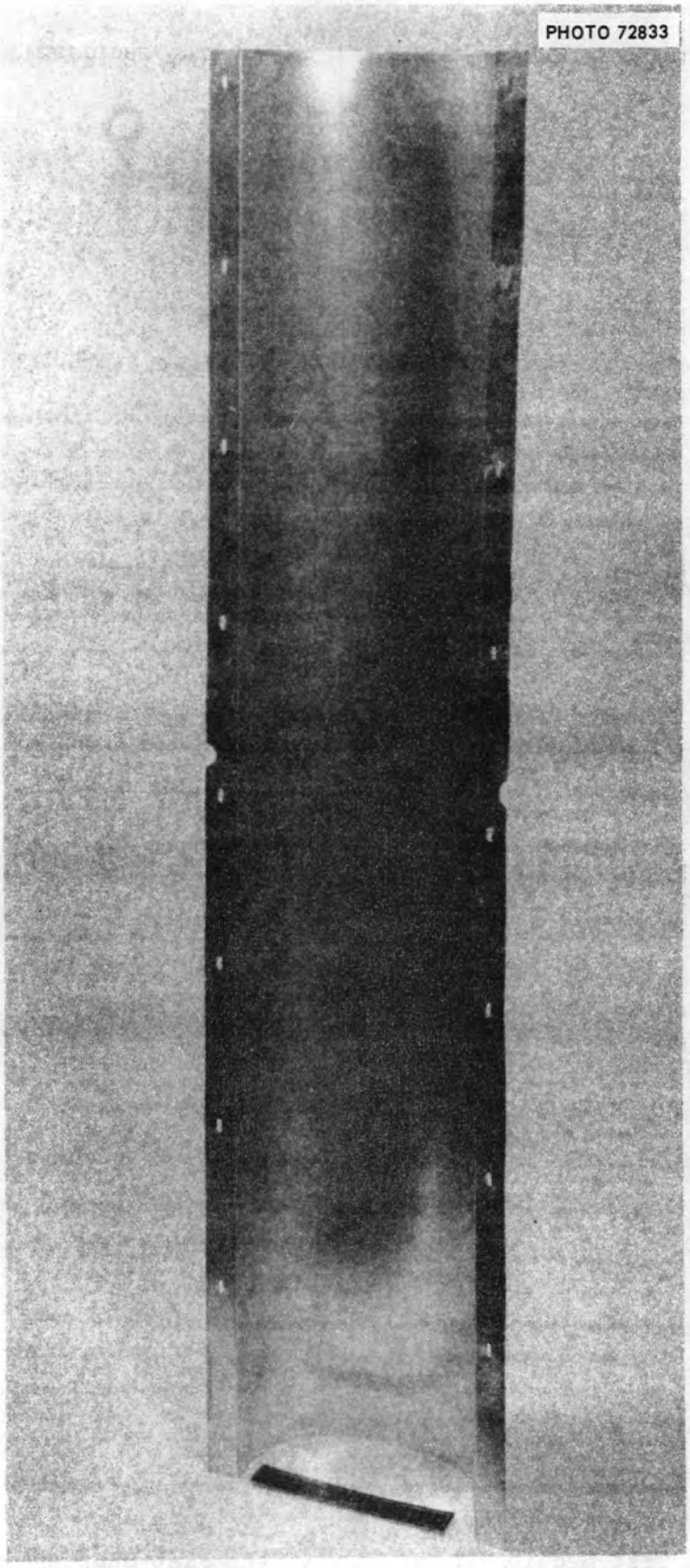

Fig. 4. Curved Shutter.

of the same design were used to collect the water leaving the top of the annulus. The water flow was controlled by globe valves in the lines from the water supply header to the inlet manifolds.

A Cenco Hyvac Model 45 mechanical vacuum pump was used to evacuate the tank. The vacuum pump was connected to the top lid of the tank with 3/4 in. copper tubing. An isolation valve was located in the line near the tank, and a venting valve was positioned on a tee off the line.

Electrical System

Electrical power was supplied to the test section from a variable transformer which had an output voltage range of 0 to 270 volts and a maximum power rating of 7.5 kva. Flexible cables connected the variable transformer to insulated binding posts which passed through the tank lid in glands sealed with O-rings. The heater leads were connected to the binding posts on the inside of the tank lid.

Instrumentation

Temperature measurements were obtained using chromel-alumel thermocouples attached to the surfaces of the test section assembly. The thermocouples were made of 0.010-in.-diam wire covered with glass insulation. The thermocouples on the heater surface and water wall were threaded through two-hole ceramic insulators, and the junctions were spot-welded to the surface. The thermocouples were supported with a wire clip placed over the ceramic insulator and spot welded to the surface at each end. The thermocouples on the reflector and shutter were attached by mounting the junction beneath the head of a No. 3 sheet metal screw threaded through the aluminum. The thermocouples were located at two axial positions 11 1/2 in. from the ends of the heated length. These axial positions were selected so that the thermocouples on the heater surface would be located midway of one of the wire coils inside the heater. There were 13 thermocouples on the heater, 4 on the reflector, 3 on the shutter, and 6 on the water wall at each of the two axial positions. The locations of the thermocouples are indicated in the schematic drawing of the test section assembly shown in Fig. 5 and in the cross section shown in Fig. 6.

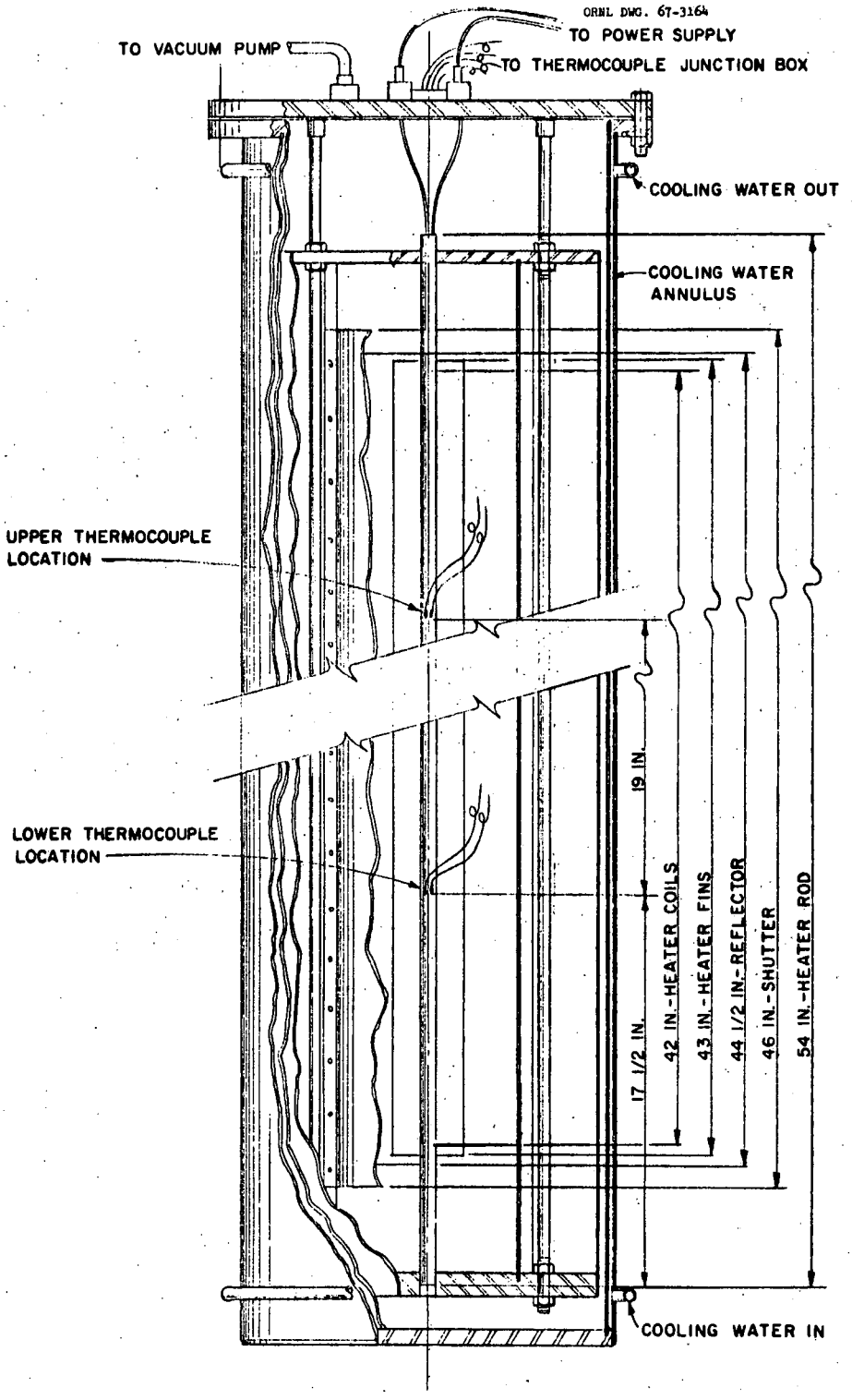

Fig. 5. Schematic Drawing of Test Assembly Installed in Vacuum Tank.

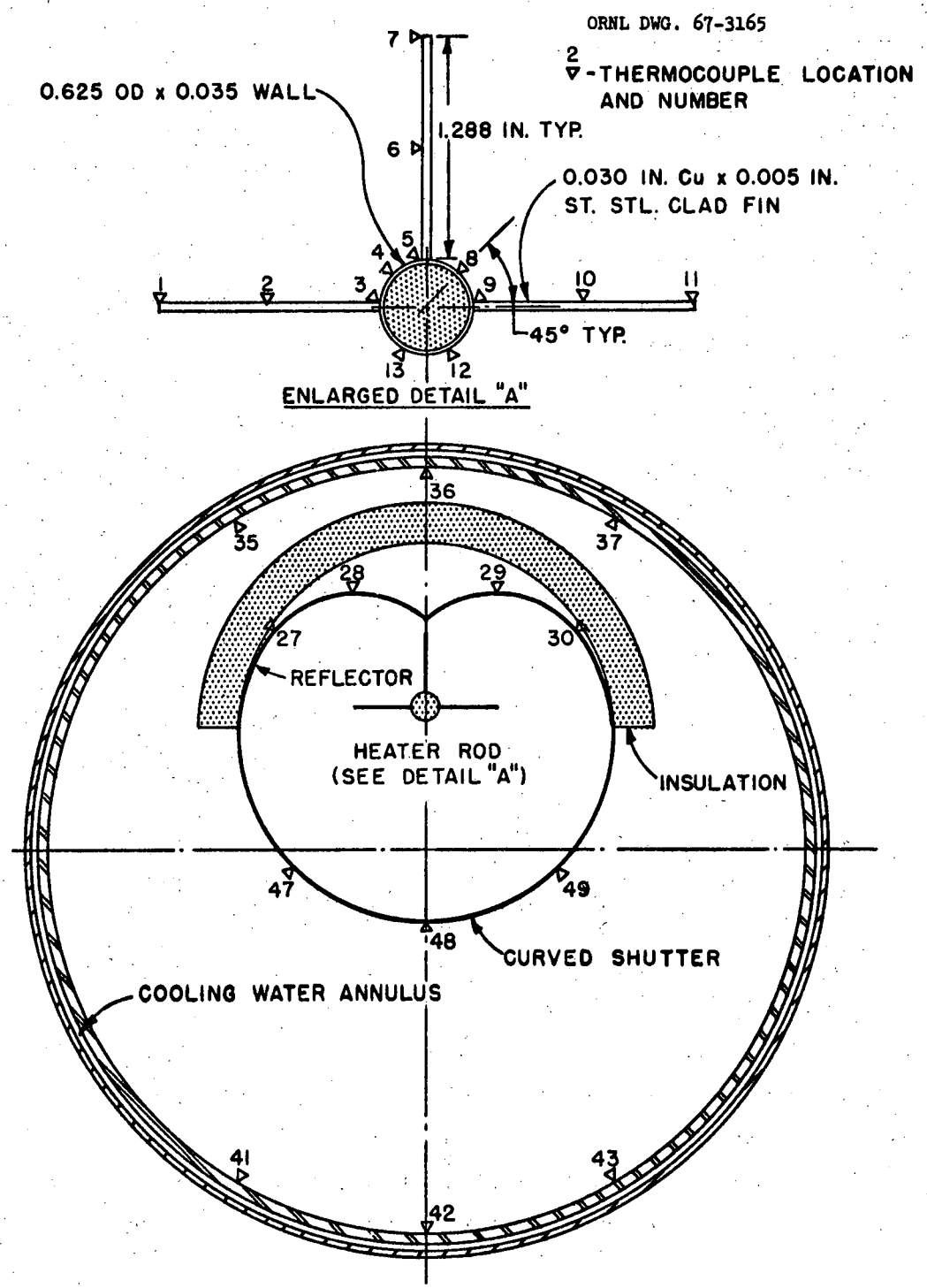

Fig. 6. Cross Section Through Assembly at the Upper Thermocouple Location.

The thermocouple wires were soldered to brass pin blocks mounted in the tank lid, and copper leads connected the pin blocks to a terminal strip. The terminal strip was mounted in a closed box and connected to a rotary switch with copper leads to the cold junction connected to the common terminals. The junction of these leads with the chromel and alumel wires of the cold junction was fastened to the tank lid at the pin blocks and insulated to cancel the thermal emf of the copper and chromel-alumel junction of the thermocouples. The thermocouple emf was measured with a precision temperature indicator, with the smallest scale division being 0.002 mv. The voltage across the heater was measured with a voltmeter using full-scale ranges of 150 and 300 volts. The current was measured with an ammeter connected to the secondary winding of a current transformer. The ratio of the primary to secondary current was 5:1. The ammeter had full-scale ranges of 2.5 and 5 amperes.

The pressure in the vacuum tank was measured with a U-tube mercury manometer and a McLeod gage. The mercury manometer had one side open to the atmosphere, and had scale divisions of 1 mm. The McLeod gage had a scale range from 0.1 to 4000 μ.

PROCEDURE

Experiments were performed on four assembly configurations at both atmospheric pressure and in a vacuum. In addition, one experiment was run with variable pressure. The conditions for the cases investigated are listed in Table 1. The shutter was removed from the assembly for the case of the "open" shutter position.

In most of the experiments data were taken at four different heat input rates. For the cases with the shutter open, the linear heat transfer rate was varied over the range from 1000 to 4400 Btu/hr-ft. For the cases with the shutter closed, the heat input rates were set to give the same fin base temperature as each of the runs with the shutter open. In

Table 1. Conditions for Test Runs

	Air Pressure	Shutter Position and Type	Reflector Insulation
1	Atmospheric	Open	Removed
2	Variable	Open	Removed
3	2 mm Hg abs	Open	Removed
4	Atmospheric	Closed (curved)	Removed
5	2 mm Hg abs	Closed (curved)	Removed
6	Atmospheric	Closed (flat)	Removed
7	2 mm Hg abs	Closed (flat)	Removed
8	Atmospheric	Open	Installed
9	2 mm Hg abs	Open	Installed

the case of variable air pressure, the heat input rate was set to give the same fin base temperature at several different pressures from 2 mm Hg abs at atmospheric.

The procedure followed was similar for each of the experiments. The following steps were typical for a run at atmospheric pressure:

1. Dry air was run into the tank while it was vented to force out moist air that might cause condensation on the water wall. This was done for several minutes, and then the air-inlet valve was closed and the air line disconnected.

2. The cooling water to the water annulus was turned on.

3. The electrical power was turned on, and the voltage was increased gradually until the desired voltage was reached.

4. The temperatures were observed until the system appeared to be at thermal equilibirum.

5. The voltage and current were read and recorded.

6. The thermocouple outputs were read and recorded.

7. The first thermocouple emf was read again and compared with the recorded value. If a change of more than 2°F occurred, the run was repeated.

8. The voltage and current were read again and compared with the recorded values.

The procedure for the vacuum runs was the same except that the vacuum pump was turned on and the tank was evacuated before either the cooling water or the electrical power was turned on. After the desired voltage was set, the pressure and temperatures were observed until the system reached equilibrium. The data were taken in the same manner as in the atmospheric runs. The lowest pressure to which the system could be pumped down was about 2 mm Hg abs, and this was the pressure at which the vacuum data were taken.

METHOD OF CALCULATION

The local radiation heat transfer rates from the tube and fins were calculated from the surface temperature data taken with the system evacuated. The effectiveness of the reflector and the total heat radiated for the assumption of a uniform temperature around the tube were calculated from the local heat transfer rates.

Local Heat Transfer Rates

The net heat flux from body 1 to body 2 by radiation may be expressed by the following relation.[5]

$$q_1 = \frac{F_{12} A_1 \sigma (T_1^4 - T_2^4)}{1 + (1/\alpha_1 - 1) F_{12} + (1/\alpha_2 - 1) F_{21}} , \qquad (1)$$

where

A_1 = area of body 1, ft^2

σ = Stefan-Boltzmann constant, 0.1713×10^{-8} $Btu/ft^2\text{-}hr\text{-}°R^4$

F_{12} = angle factor for radiation from body 1 to 2

F_{21} = angle factor for radiation from body 2 to 1

T_1 = temperature of body 1, °R

T_2 = temperature of body 2, °R

α_1 = absorbtivity of body 1

α_2 = absorbtivity of body 2

The angle factors F_{12} and F_{21} may be related by the following equation.[5]

$$A_1 F_{12} = A_2 F_{21} \qquad (2)$$

or

$$F_{21} = \frac{A_1}{A_2} F_{12} . \qquad (3)$$

If we assume "gray" surfaces for bodies 1 and 2, then the absorbtivity, α, is equal to the emissivity, ϵ. Substituting ϵ for α and combining Eqs. (1) and (3) yields

$$q_1 = \frac{F_{12} A_1 \sigma (T_1^4 - T_2^4)}{1 + (\frac{1}{\epsilon_1} - 1) F_{12} + (\frac{1}{\epsilon_2} - 1) F_{12} \frac{A_1}{A_2}} , \qquad (4)$$

or rearranging

$$q_1 = \frac{A_1 \sigma (T_1^4 - T_2^4)}{\frac{1}{F_{12}} + (\frac{1}{\epsilon_1} - 1) + (\frac{1}{\epsilon_2} - 1) \frac{A_1}{A_2}} . \qquad (5)$$

The tube surface was divided into 24 regions, and each side of the three fins was divided into five regions in a transverse plane. The local heat transfer rates on the front side of the tube, which has a direct view of the water wall, were calculated by the equation

$$q_n = \frac{A_N \sigma (T_N^4 - T_W^4)}{\frac{1}{F_{NW}} + (\frac{1}{\epsilon_T} - 1) + (\frac{1}{\epsilon_W} - 1) \frac{A_F}{A_W}} , \qquad (6)$$

where

A_N = area of the local region, ft^2
A_F = area of the front side of the heater rod and fins, ft^2
A_W = area of the water wall, ft^2
T_N = average temperature of the local region, °R
T_W = temperature of the water wall, °F
F_{NW} = angle factor of local region to water wall
ϵ_T = emissivity of heater surface
ϵ_W = emissivity of water wall

The local heat transfer rates on the back side of the type which faces the reflector were calculated as though the reflector were perfect, that is as though that side of the tube were radiating directly to the water wall. This was expressed by

$$q_n = \frac{A_N \sigma (T_N^4 - T_W^4)}{\frac{1}{F_{NW}} + (\frac{1}{\epsilon_T} - 1) + (\frac{1}{\epsilon_W} - 1) \frac{A_B}{A_W}} \qquad (7)$$

where

A_B = area of the back side of the heater rod and fins.

The other terms are as defined in Eq. (6).

The method of calculation of the local angle factors is given in Appendix A. The emissivity of the ceramic coating, PT-404-A, was measured

over a wide temperature range at ORNL. The variation with temperature was small, and the average value from the tests of 0.89 was used for these calculations with little error being introduced.

Reflector Effectiveness

The reflector effectiveness, E, is defined as the ratio of the heat actually radiated from the back side of the tube, q_B, to the heat which would be radiated directly to the water wall with the reflector removed, q_D. This is expressed by

$$E = \frac{q_B}{q_D} \quad . \tag{8}$$

The actual heat radiated from the back side of the tube was calculated by subtracting the heat calculated as radiated from the front side of tube, q_F, from the total heat rate for the tube, q_T, or

$$q_B = q_T - q_F \quad . \tag{9}$$

The apparent reflectivity, R, of the reflector is defined as the ratio of the heat reflected from the back side of the tube, q_R, to the heat which would be radiated directly to the water wall with the reflector removed, q_D. This is expressed by

$$R = \frac{q_R}{q_D} \quad . \tag{10}$$

The heat reflected was calculated to be the difference between the heat actually radiated from the back side of the tube and the heat absorbed by the reflector and re-radiated to the water wall, q_A, or

$$q_R = q_B - q_A \quad . \tag{11}$$

The heat absorbed and re-radiated is the sum of two terms: the heat radiated from the front of the reflector, q_{AF}, and the heat radiated from the back of the reflector, q_{AB}.

The net heat radiated from the front of the reflector was calculated by the equation

$$q_{AF} = \frac{F_{RW} A_R \sigma T_R^4 - F_{WR} A_W \sigma T_W^4}{1 + F_{RW} (\frac{1}{\epsilon_{RF}} - 1) + F_{WR} (\frac{1}{\epsilon_W} - 1)} , \qquad (12)$$

where

A_R = area of the front side of the reflector, ft^2
A_W = area of the water wall, ft^2
T_R = temperature of the reflector, °R
T_W = temperature of the water wall, °R
F_{RW} = angle factor from the front side of reflector to water wall
F_{WR} = angle factor from the water wall front side of reflector
ϵ_{RF} = emissivity of the front side of reflector
ϵ_W = emissivity of the water wall

The angle factors, F_{RW} and F_{WR}, were taken as 0.5 and 1.0, respectively. The emissivity of the Alzak coating on the front of the reflector was taken to be 0.6 on the basis of the information provided on the emissivity of this type of coating given in Ref. 6.

The net heat radiated from the back of the reflector was assumed to be zero for the case with the reflector back insulated. For the case with the back of the reflector bare, the net heat radiated from the back side of the reflector was calculated by

$$q_{AB} = \frac{A_{RB} \sigma (T_R^4 - T_W^4)}{\frac{1}{\epsilon_R} - (\frac{1}{\epsilon_W} - 1) \frac{A_{RB}}{A_{WB}}} , \qquad (13)$$

where

A_{RB} = area of the back side of the reflector, ft^2

A_{WB} = area of the water wall behind the reflector, ft^2

T_R = temperature of the reflector, °F

T_W = temperature of the water wall, °R

ϵ_R = emissivity of the back side of reflector

ϵ_W = emissivity of the water wall

Heat Transfer Rate for a Uniform Tube Temperature

The heat transferred by radiation from the finned tube was calculated for the ideal case of uniform surface temperature around the tube. This was done by calculating the heat dissipated from the tube surface at a given temperature and adding to that quantity the heat dissipated from the fin surfaces at a fin-base temperature equal to the given tube temperature. The finned-tube surface was divided into five elements: the front side of the tube, the back side of the tube, the front of the two side fins, the back of the two side fins, and the rear fin. The total heat dissipated, q_T, is then expressed by

$$q_{TOTAL} = q_{TF} + q_{TB} + q_{SFF} + q_{SFB} + q_{RF} \quad . \tag{14}$$

The heat radiated from the front side of the tube at uniform temperature was calculated from an overall radiation constant, K_{TF}, obtained by summing up the coefficients of the fourth-power temperature difference for the 12 regions of the front side of the tube. Then the heat dissipated from the front side of the tube is given by

$$q_{TF} = K_{TF} \left(T^4 - T_W{}^4\right) \quad , \tag{15}$$

where

T = temperature of the tube

T_W = temperature of the water wall

The heat radiated from the back side of the tube was calculated in the same manner except that the reflector effectiveness was used as a factor in the equation. The reflector effectiveness was plotted as a function of the average fin-base temperature, and the value used for the back side of the tube was taken at the fin-base temperature corresponding to the uniform tube surface temperature. This was expressed by the relation

$$q_{TB} = K_{TB} E_T (T^4 - T_W^4) \quad . \tag{16}$$

The amounts of heat radiated from the front of the side fins, the back of the side fins, and the rear fin were each plotted as a function of the base temperature of the particular fin. The heat radiated from each of these surfaces for an arbitrary, uniform tube temperature was read from the curves at that value of fin-base temperature.

RESULTS AND DISCUSSION

The results of the experiments are presented in several forms. Graphs were plotted to show the temperature distribution on the radiator tube and fins for a typical case, the linear heat transfer rate (heat transfer per foot of tube) as a function of temperature, and the heat removed by convection as a function of test chamber air pressure and fin-base temperature. The calculated results are presented in graphs showing the reflectivity and reflector effectiveness as a function of fin-base temperature and the linear heat transfer rate as a function of tube surface temperature for the ideal case of uniform tube temperature.

Temperature Distribution on Radiator Tube and Fins

The temperature distribution on the radiator tube and fins for the case of the shutter open, uninsulated reflector, at a heat rating of 4424 Btu/hr-ft in a vacuum, is shown in Figs. 7 and 8. This distribution is typical of those found in each of the experiments. The tube temperature

ORNL DWG. 67-3166

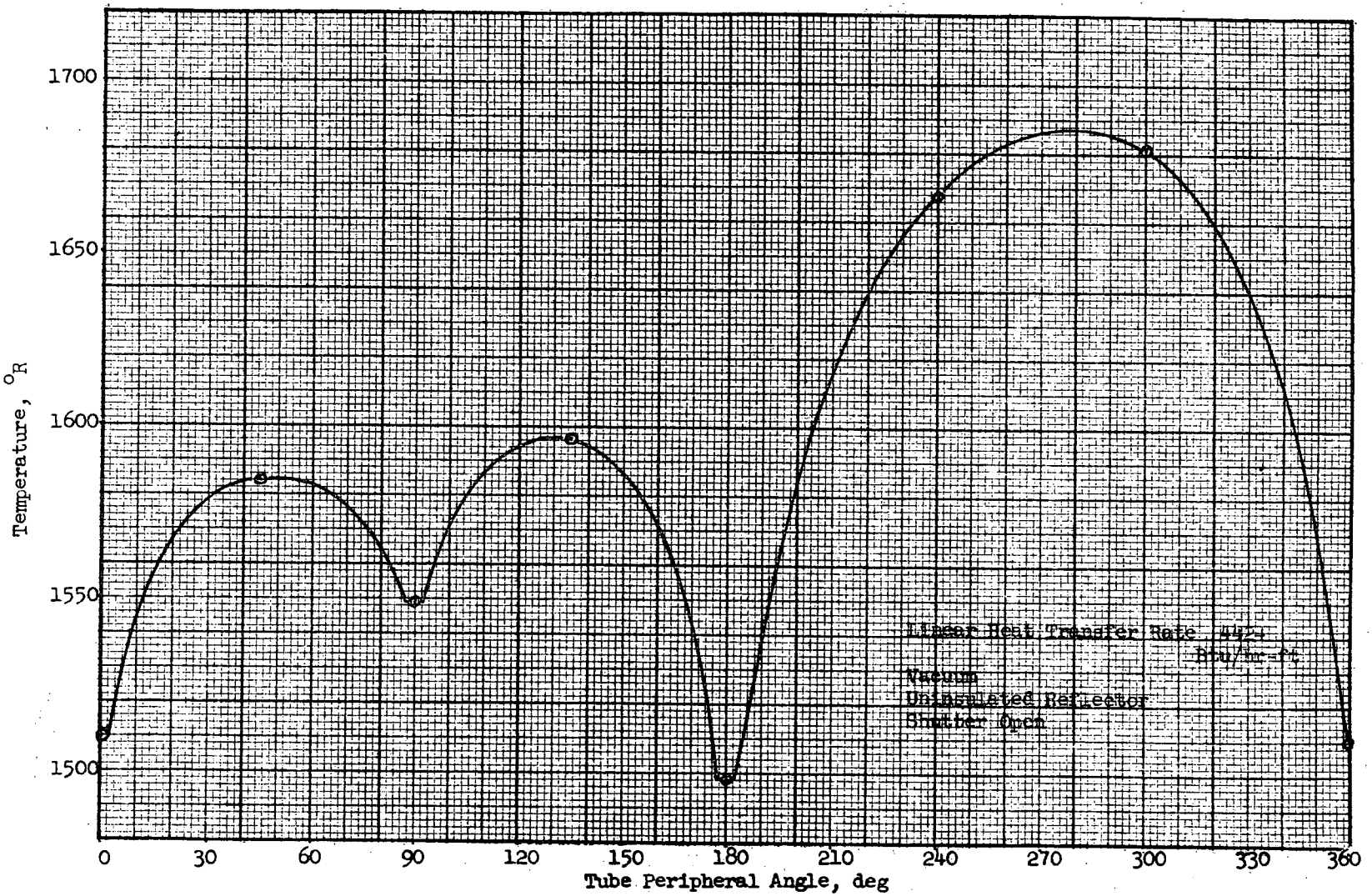

Fig. 7. Typical Tube Temperature Distribution.

ORNL DWG. 67-3167

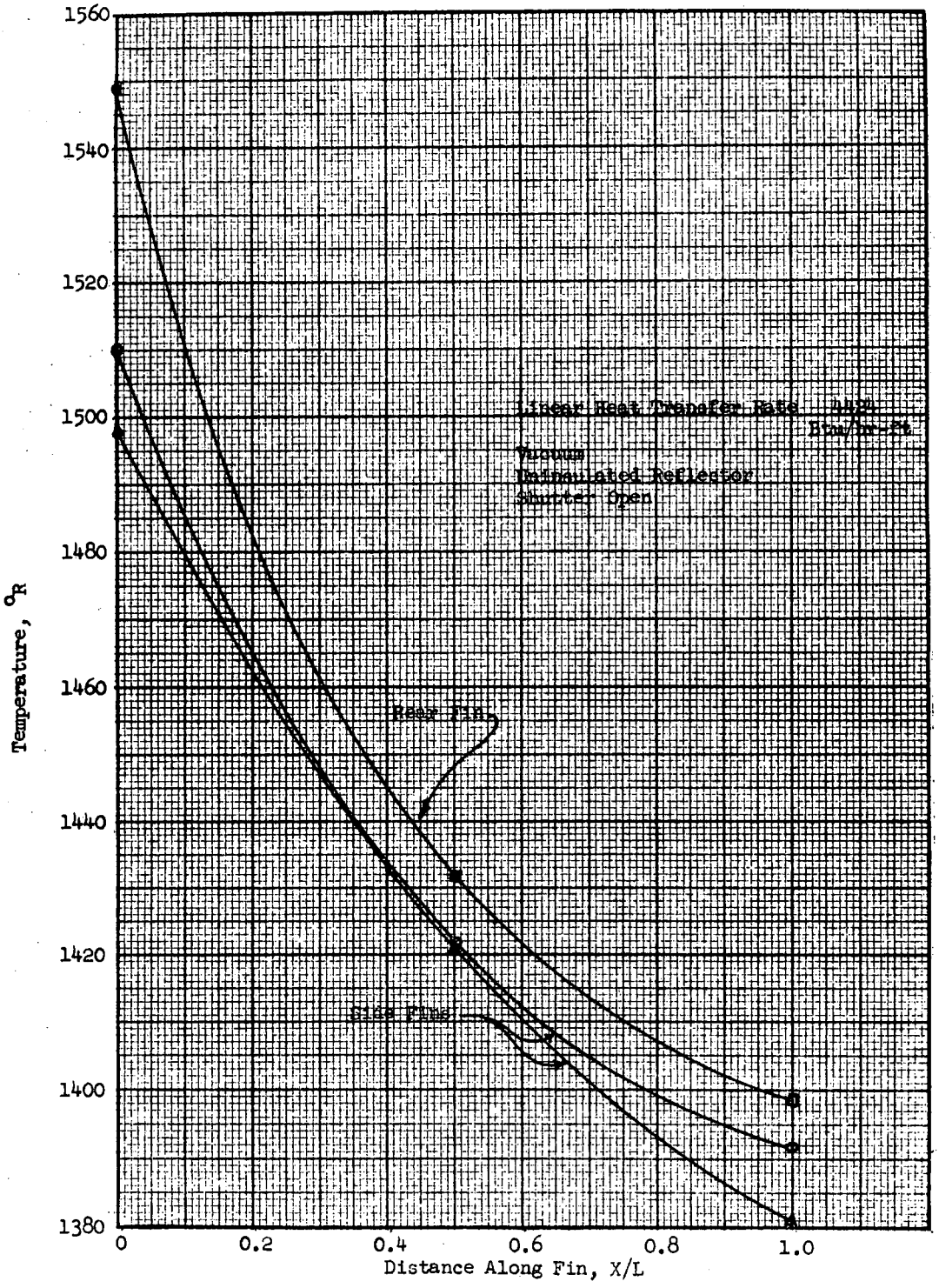

Fig. 8. Typical Temperature Distribution on Fins.

varied from 1498°R at the fin base to 1686°R on the front size, opposite the fins. This variation occurs because most of the heat is removed from the fins and the heat generation rate is essentially constant around the tube. This large variation would not be expected to occur on the LPS radiator tubes with potassium vapor condensing at constant temperature and a small temperature difference between the potassium vapor and the tube wall. Thus the actual condenser tube wall would tend to run at a uniform temperature. The temperature at the base of the rear fin on the heater rod was higher than that of the side fins because the entire surface of the rear fin was radiating to the reflector and only one side of the side fins was doing so. The temperature difference between the base and the tip of the side fins was 118°F.

Variation of Heat Transfer Rate on Radiator Tube and Fins

The heat transfer rate per unit area and the temperature were plotted in Fig. 9 as a function of the distance along the surface from the point at the center of the front of the tube for one-half of the radiator tube. The heat transfer rate peaks sharply on the tube surface where the surface temperature is higher. These local peaks have only a small effect on the average heat flux and temperature, however, since the surface area of the tube is small compared to the surface area of the fins. Consequently, the average heat flux and temperature is only slightly higher than the average values for the fin surfaces.

Thermal Performance

The thermal performance of the radiator tube was correlated on the basis of the average of the temperatures measured at the bases of the three fins. The fin-base temperature was selected as the parameter to be used to correlate the heat transfer because the heat removal capability of the fins is a function of this temperature alone for a given combination of geometry and meterials. The performance of the LPS radiator tube can then be related directly to the fin-base temperature, which is nearly equal to the temperature of the potassium condensing inside the tube.

ORNL DWG. 67-3168

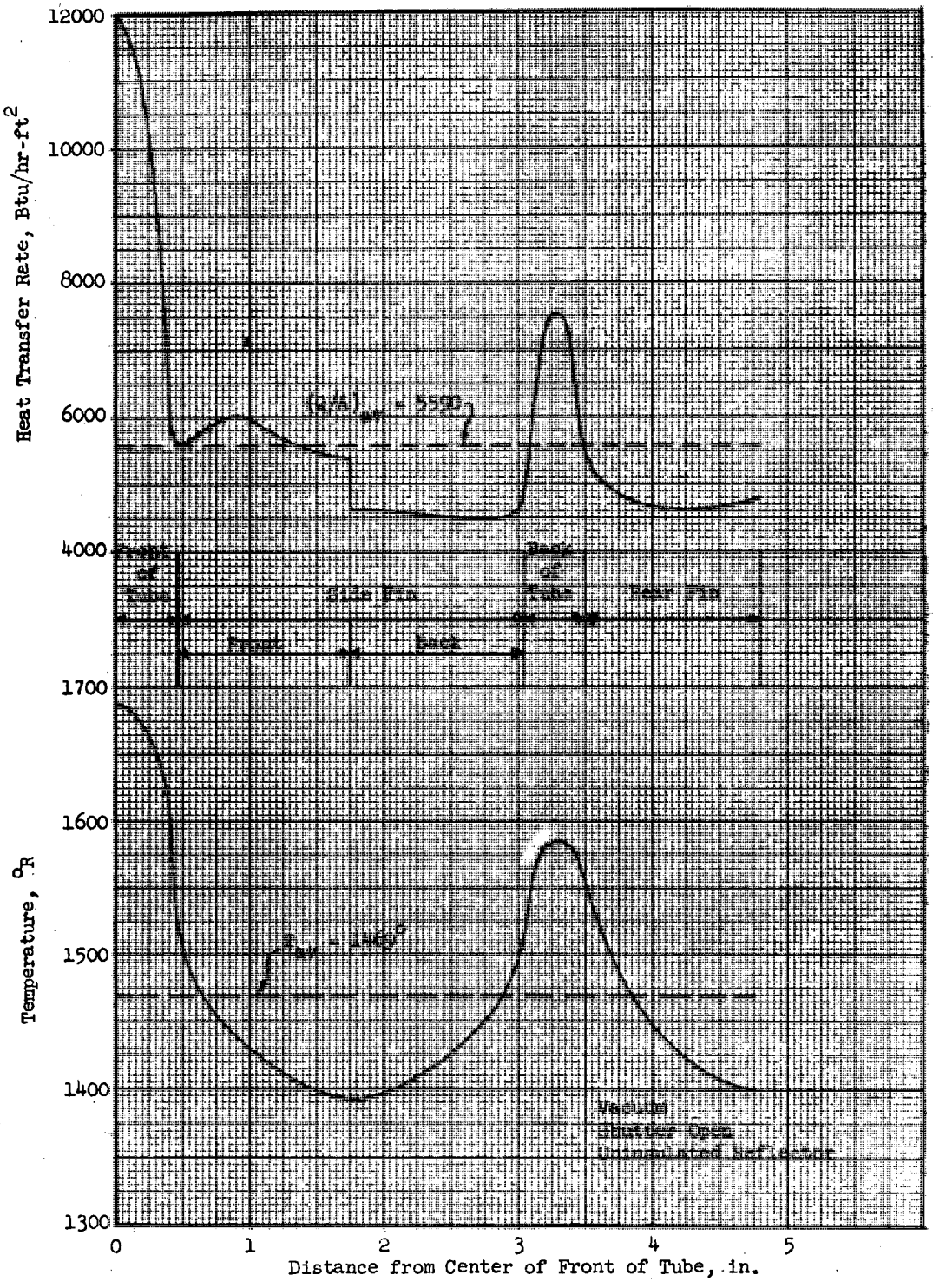

Fig. 9. Heat Transfer Rate and Temperature vs Distance from Center of Front of Tube on One-half of Radiator Tube and Fin Surface.

Heat Transfer in a Vacuum

The linear heat transfer rate in a vacuum is shown for three cases in Fig. 10. For the reference case, with the shutter open and the reflector uninsulated, the LPS design heat load of 4265 Btu/hr-ft was achieved at an average fin-base temperature of 1510°R. The data for the reference case was correlated by the following equation:

$$q = 2.528 \times 10^{-11} T^{5.5} \quad , \tag{17}$$

where

q = linear heat transfer rate, Btu/hr-ft

T = average fin-base temperature, °R

Effects of Closed Shutter. The heat transfer rate with the shutter closed in a vacuum is plotted on the lower curve of Fig. 10. Both the curved and flat shutter gave the same results in a vacuum. The shutter was quite effective in reducing the heat dissipated from the radiator tube for a given fin-base temperature. The linear heat transfer rate was reduced to 1700 Btu/hr-ft at the full-load temperature of 1510°R, or to about 40% of the full heat load. At 60% of full load, the temperature was reduced to only 1060°R.

Effects of Thermal Insulation on Back of Reflector. The heat transfer rate with the back of the reflector insulated and the shutter open in a vacuum is plotted on the middle curve of Fig. 10. These are approximately the conditions that would be encountered in space applications of the LPS radiator. The design heat load was achieved at an average fin-base temperature of 1545°R, or 35°F hotter than with the uninsulated reflector at the design heat load.

ORNL DWG. 67-3169

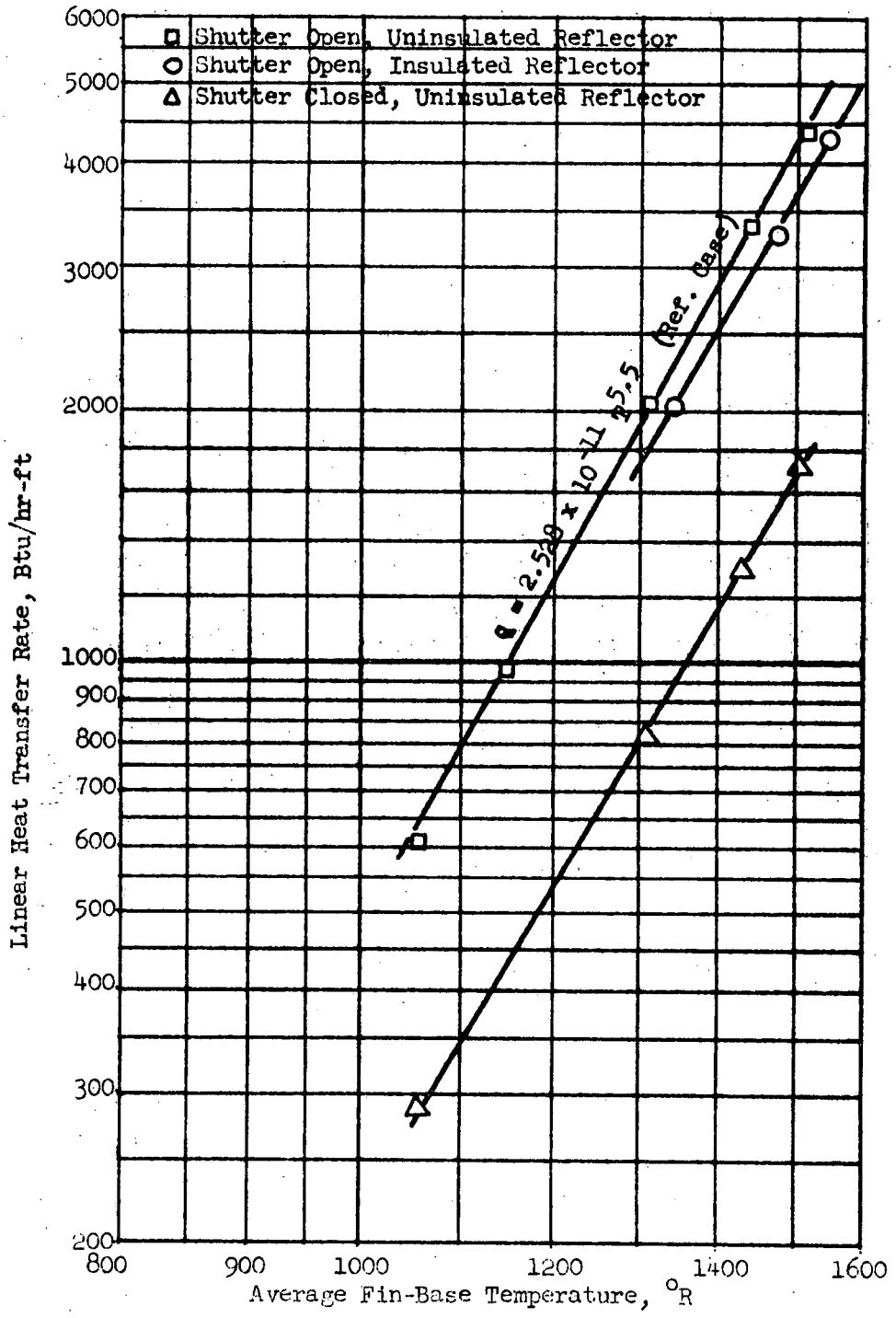

Fig. 10. Linear Heat Transfer Rate vs Average Fin-Base Temperature in a Vacuum.

Heat Transfer at Atmospheric Pressure

The heat transfer performance at atmospheric pressure is presented in Fig. 11. The curve for the reference case (with the shutter open and uninsulated reflector) in a vacuum is given for comparison. The average fin-base temperature used to correlate the data was taken from the temperatures measured with the lower set of thermocouples. The temperatures were lower at the bottom end of the test assembly than at the top because of the temperature rise in the air in the thermal convection currents. The design heat load was rejected at a temperature of 1425°R with the reflector uninsulated and the shutter open. This temperature is 85°F less than for the reference case at design heat load.

Effects of Closed Shutter. The heat transfer rate is shown for both the curved and flat shutter closed with the uninsulated reflector at atmospheric pressure in Fig 11. The lowest curve is for the flat shutter closed with baffles closing off the ends of the reflector to reduce thermal convection. The linear heat transfer rate was reduced to 2000 Btu/hr-ft at a temperature of 1425°R, which corresponds to the full-load temperature with the shutter open. The next higher curve is for the case with the curved shutter closed. The heat transfer rate was 2300 Btu/hr-ft at 1425°R. The performance of the two shutters approached the same value as the heat load was reduced. The temperature was 860°R at 6% of design heat load with either shutter closed.

Effects of Insulated Reflector. The linear heat transfer rate for the case with the back of the reflector insulated with the shutter open at atmospheric pressure is plotted on the next curve above the line for the reference case. The conditions for this case are similar to those that would exist with no cooling on the inside water-wall of the LPS radiator. The temperature at the design heat load was 1443°R, which is only 18° hotter than for the case with the reflector uninsulated.

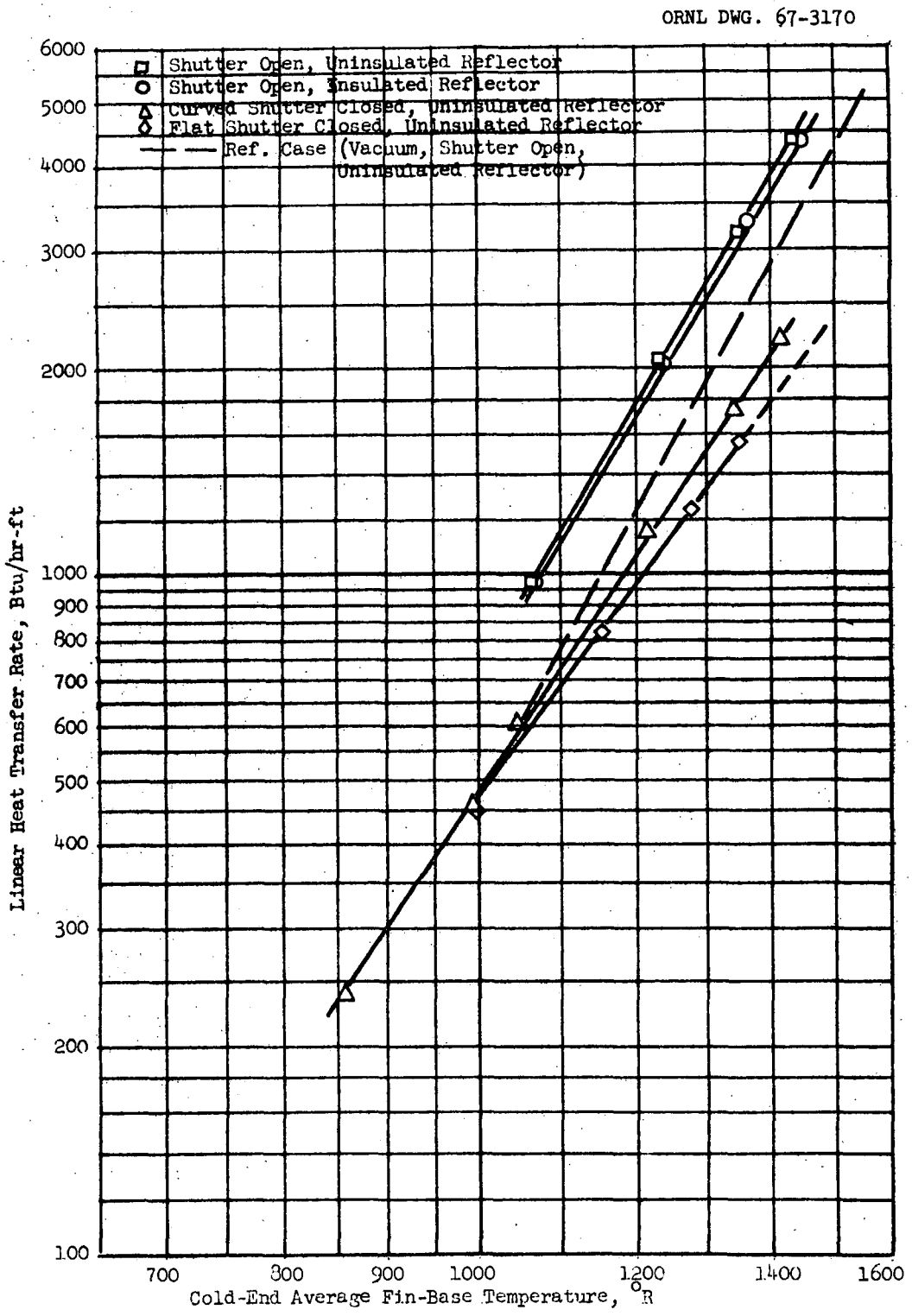

Fig. 11. Linear Heat Transfer Rate vs Cold-End Average Fin-Base Temperature at Atmospheric Pressure.

Reflector and Shutter Temperature

The temperature of the reflector and the shutter is shown in Fig. 12 for the cases with the curved shutter closed and the reflector uninsulated in a vacuum and at atmospheric pressure. The average fin-base temperature is shown also for comparison. The solid lines are for the vacuum case, and the dashed lines are for atmospheric pressure. The reflector temperature was 964°R, and the shutter temperature was 1050°R for the vacuum case at 1700 Btu/hr-ft, at which time the fin-base temperature was 1510°R. For the atmospheric pressure case, the reflector temperature was 875°R and the shutter temperature was 856°R at 2300 Btu/hr-ft. The fin-base temperature was 1425°R at this power level.

The average temperature of the reflector at the upper thermocouple location for six cases is shown in Fig. 13. The solid lines are for the vacuum cases, and the dashed lines are for those at atmospheric pressure. The reflector temperature was 860°R with the reflector uninsulated, and 1058°R with the reflector insulated, with the shutter open at the design heat load in a vacuum. The temperature was 795°R and 910°R, respectively, for the same configurations at the design heat load at atmospheric pressure.

Convection Heat Transfer vs Air Pressure

The heat removed by thermal convection vs the absolute air pressure in the vacuum tank is shown in Fig. 14. These data were taken with the shutter open and the reflector uninsulated, with the temperature at the base of one side fin maintained at 1062°R for each pressure. It was then assumed that the heat transferred by radiation was constant with pressure. The heat removed by convection was assumed to be negligible at the lowest pressure in the tank which was 2 mm Hg abs, and the radiant heat was taken as the total at this pressure. The heat removed by convection at higher pressures was found from the difference between the total heat and the radiant heat. The heat removed by thermal convection appears to be a linear function of pressure. This indicates that the contribution of convection to the heat transfer is negligible at a pressure of 2 mm Hg absolute, and that the experiments run at that pressure had, for all practical purposes, heat transfer by radiation only.

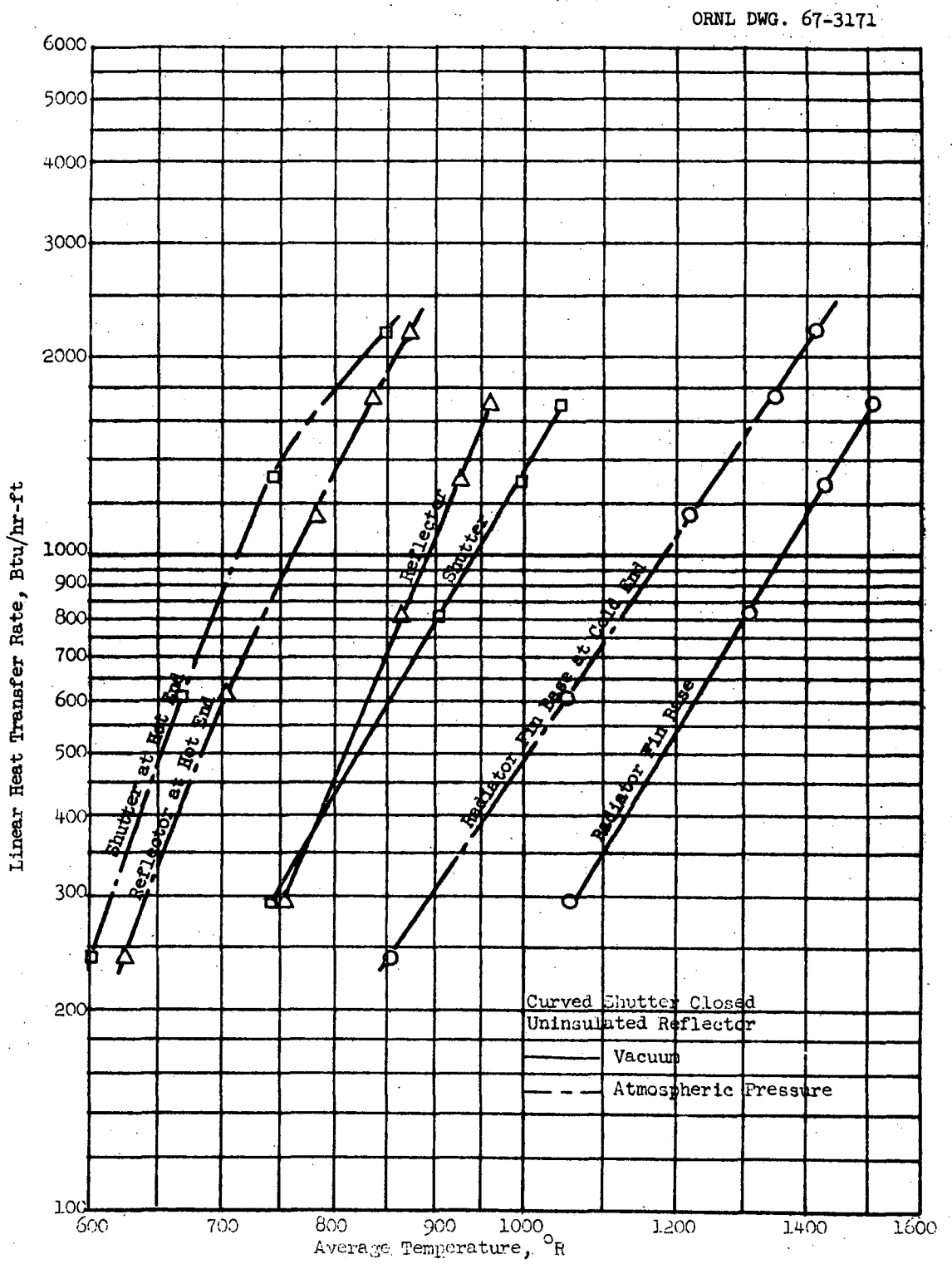

Fig. 12. Linear Heat Transfer Rate vs Average Temperature of Radiator Fin-Base, Shutter and Reflector with Curved Shutter Closed.

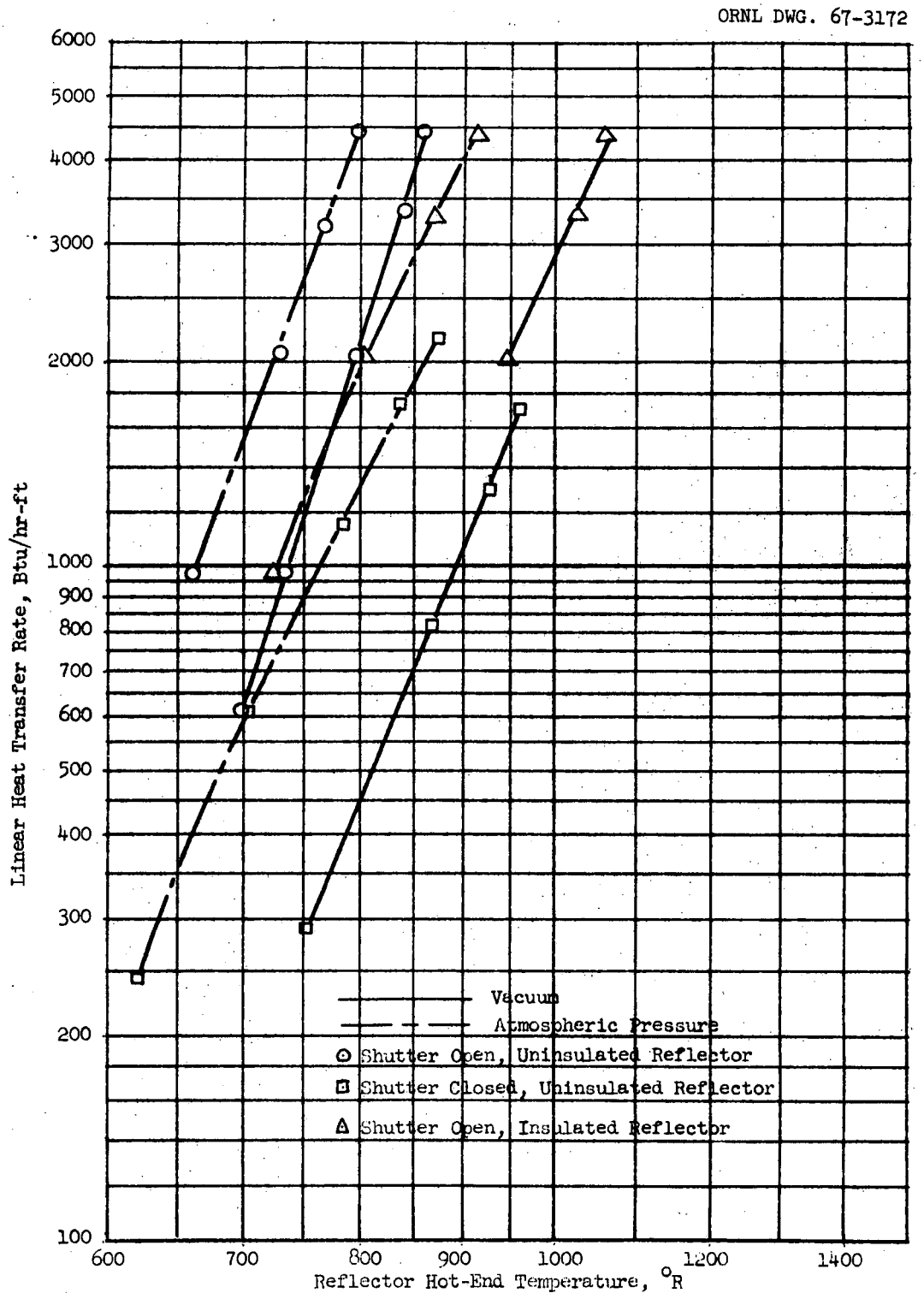

Fig. 13. Linear Heat Transfer Rate vs Reflector Hot-End Temperature.

ORNL DWG. 67-3173

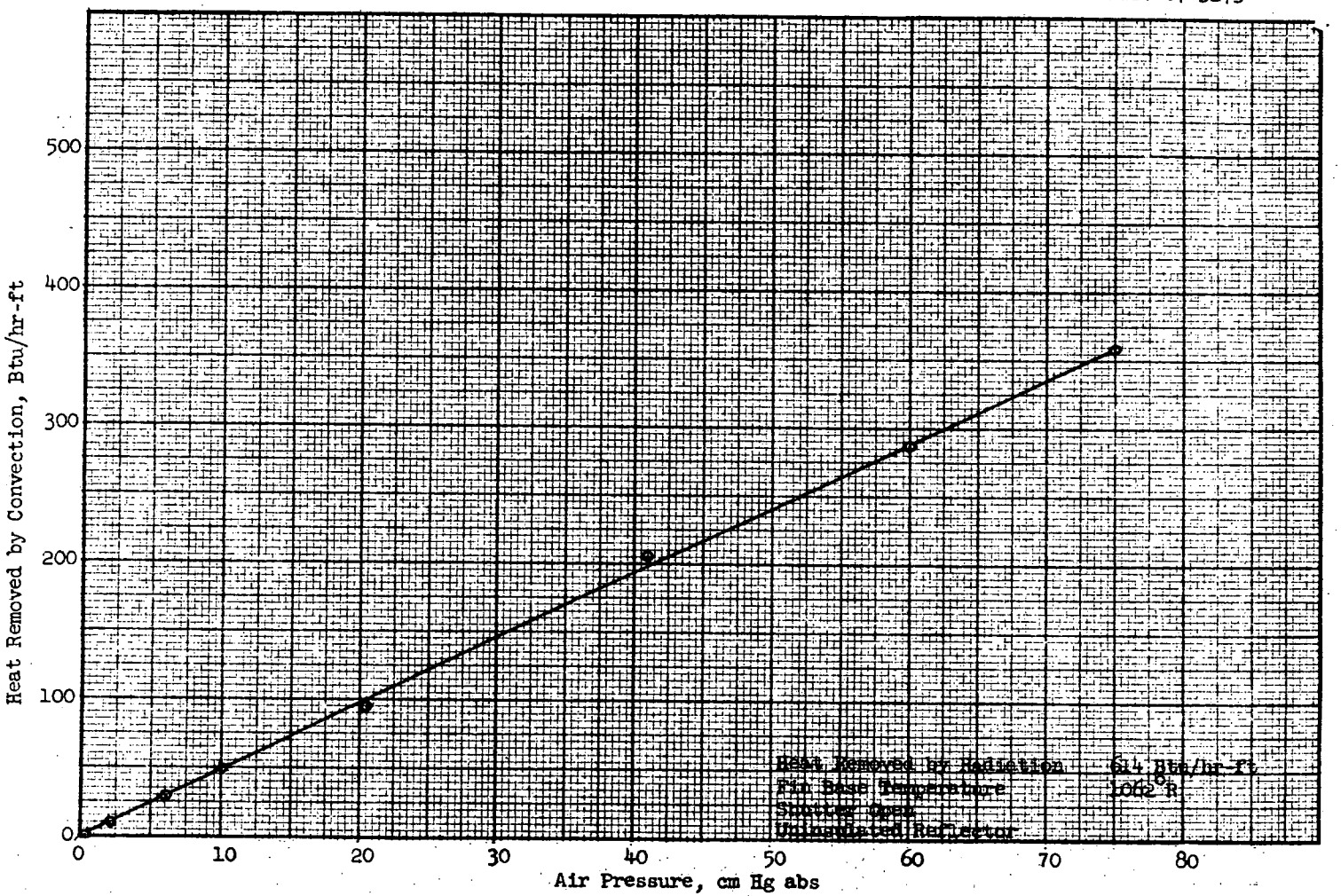

Fig. 14. Heat Removed by Convection vs Air Pressure at Constant Fin-Base Temperature.

Convection Heat Transfer vs Temperature

The heat removed by thermal convection as a function of the average fin-base temperature of the lower set of thermocouples is presented in Fig. 15. These data were taken with the shutter open and the reflector uninsulated. The heat removed by convection was calculated by taking the difference between the heat transfer rate at atmospheric pressure and that in a vacuum at the same average fin-base temperature. The contribution to the total heat transfer by convection was found to vary from 33% at 1100°R to 24% at 1450°R.

Calculated Results

Local Heat Transfer Rates

The calculated local heat transfer rates for the radiator tube and fins with the uninsulated reflector and the shutter open in a vacuum for a measured heat input of 4424 Btu/hr-ft are listed in Table 2. The tube surface was divided into 15° segments, and the heat transfer rate was calculated using the temperature at the midpoint of the segments. The fins covered an angle of 7.5°, and segments of 11.25° were used adjacent to the fins. The heat transfer rate for a 15° segment varied from 45.6 Btu/hr-ft near a fin to 81.9 Btu/hr-ft at the highest temperature on the front side of the tube. The fins were divided into five sections, and the heat transfer rate was calculated from the temperature at the midpoint of the sections. The heat transfer rate was calculated separately for the front and back sides of the side fins. The two sides of the rear fin were combined. The heat transfer on the front of the side fin was about 25% higher than on the back side. This is because of the smaller angle factors on the back side. The heat transfer rate remains nearly constant as one moves radially outward along the fin. The decrease in temperature is offset by the increase in the angle factor so that the fin is about equally effective in emitting heat at each point along its length. The variation in the local heat transfer rate for this case is typical for all of the cases analyzed.

Table 2. Calculated Local Heat Transfer Rates for A Measured Heat Input of 4424 Btu/hr-ft with Bare Reflector and Shutter Open in a Vacuum

Tube		Fins	
Peripheral Tube Angle (deg)	Linear Heat Transfer Rate (Btu/hr-ft)	X/L	Linear Heat Transfer Rate (Btu/hr-ft)
9.375	26.8	Front of Side Fin	
22.5	45.6	0.1	122.6
37.5	50.9	0.3	129.1
52.5	51.2	0.5	124.2
67.5	46.6	0.7	119.3
80.625	28.2	0.9	116.0
99.375	28.7	Back of Side Fin	
112.5	47.7	0.1	96.6
127.5	52.8	0.3	96.0
142.5	52.4	0.5	97.3
157.5	46.0	0.7	98.0
170.625	26.6	0.9	98.9
189.375	26.4	Rear Fin	
202.5	49.4	0.1	212.0
217.5	62.5	0.3	202.0
232.5	72.5	0.5	200.2
247.5	78.2	0.7	200.6
262.5	81.1	0.9	202.0
277.5	81.9	Front of Side Fin	
292.5	78.4	0.1	123.2
307.5	75.6	0.3	130.2
322.5	66.4	0.5	123.8
337.5	53.5	0.7	117.6
350.625	28.9	0.9	112.9
		Back of Side Fin	
		0.1	97.2
		0.3	96.9
		0.5	97.0
		0.7	96.6
		0.9	96.3
Total	1258.0	Total	3206.0
Total 4464 Btu/hr-ft			

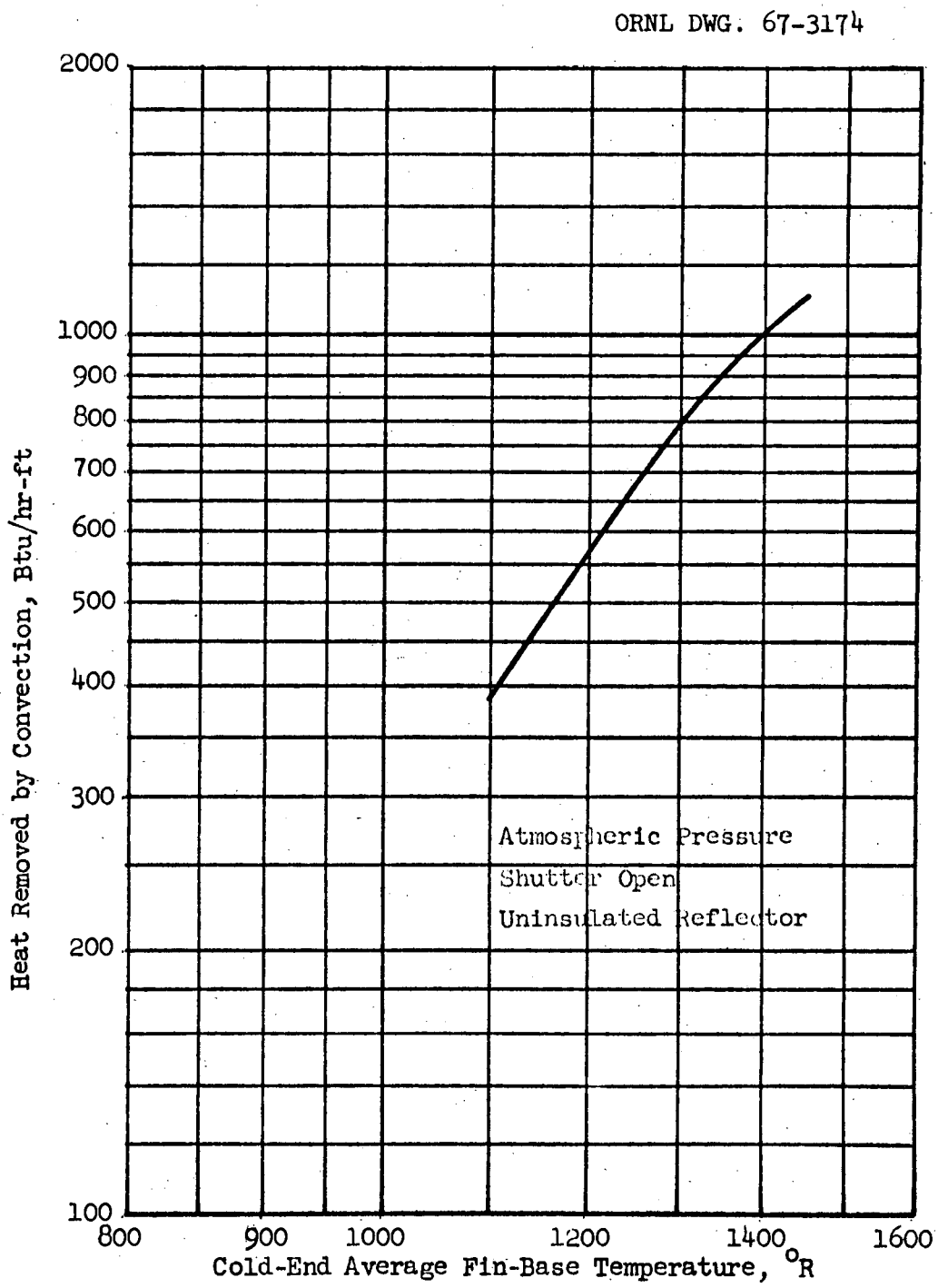

Fig. 15. Heat Removed by Convection vs Cold-End Average Fin-Base Temperature.

Reflector Effectiveness

The apparent reflectivity of the reflector both insulated and uninsulated with the shutter open in a vacuum is shown in Fig. 16 as a function of the fin-base temperature. For the case with the back of the reflector insulated, the reflectivity was found to be 54.5% at 1510°R. The reflectivity was 67% at the same fin-base temperature with the reflector uninsulated. The difference in the reflectivity for the two cases is probably because of the dependence of the reflectivity upon the temperature of the radiation source and of the reflector itself. The reflector was at a higher temperature with the back insulated than without the insulation. The reflectivity was calculated to be 78% when receiving energy from a black body with a Maxwell-Boltzmann distribution of energy with wave-length at a temperature of 1510°R. This calculation was based on the reflectivity of the Alzak process aluminum as a function of source wave-length given in Ref. 6. This is based on data taken where the reflector was at near room temperature. It would appear that while the reflectivity increases with increasing source temperature, as the temperature of the reflector increases with a constant source temperature the reflectivity decreases.

Another effect may have caused the reflectivity to be lower when the reflector operated at a higher temperature. Crazing of the Alzak surface was observed after having run the reflector above 860°R. Although the cracks formed were very fine and no apparent damage was done to the bond between the aluminum oxide and the metal, the surface may have become more diffuse in nature and yielded a lower reflectivity. This surface crazing may account for the much greater decrease in reflectivity with lower fin-base temperatures than calculated from the variations in reflectivity with source wave-length. The surprisingly low value of 33% was found for the uninsulated reflector at 1320°R as compared to a calculated value of 76%.

The reflector effectiveness, which is defined in the Method of Calculation section, is shown for the same two cases in Fig. 17. Since the effectiveness includes both the reflection and the emission from the reflector surfaces, it was significantly influenced by the insulating of the

ORNL DWG. 67-3175

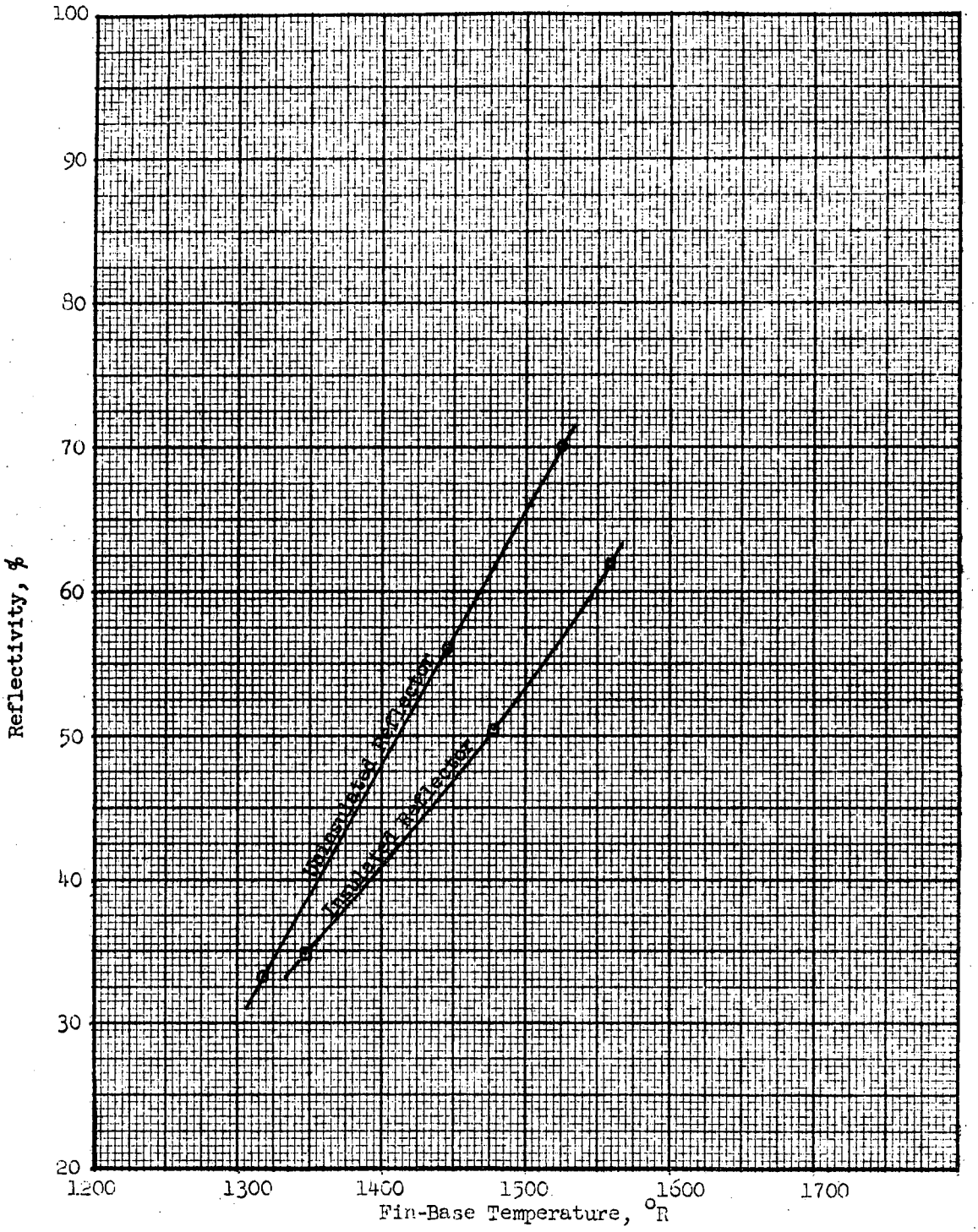

Fig. 16. Reflectivity vs Fin-Base Temperature with Shutter Open in a Vacuum.

ORNL DWG. 67-3176

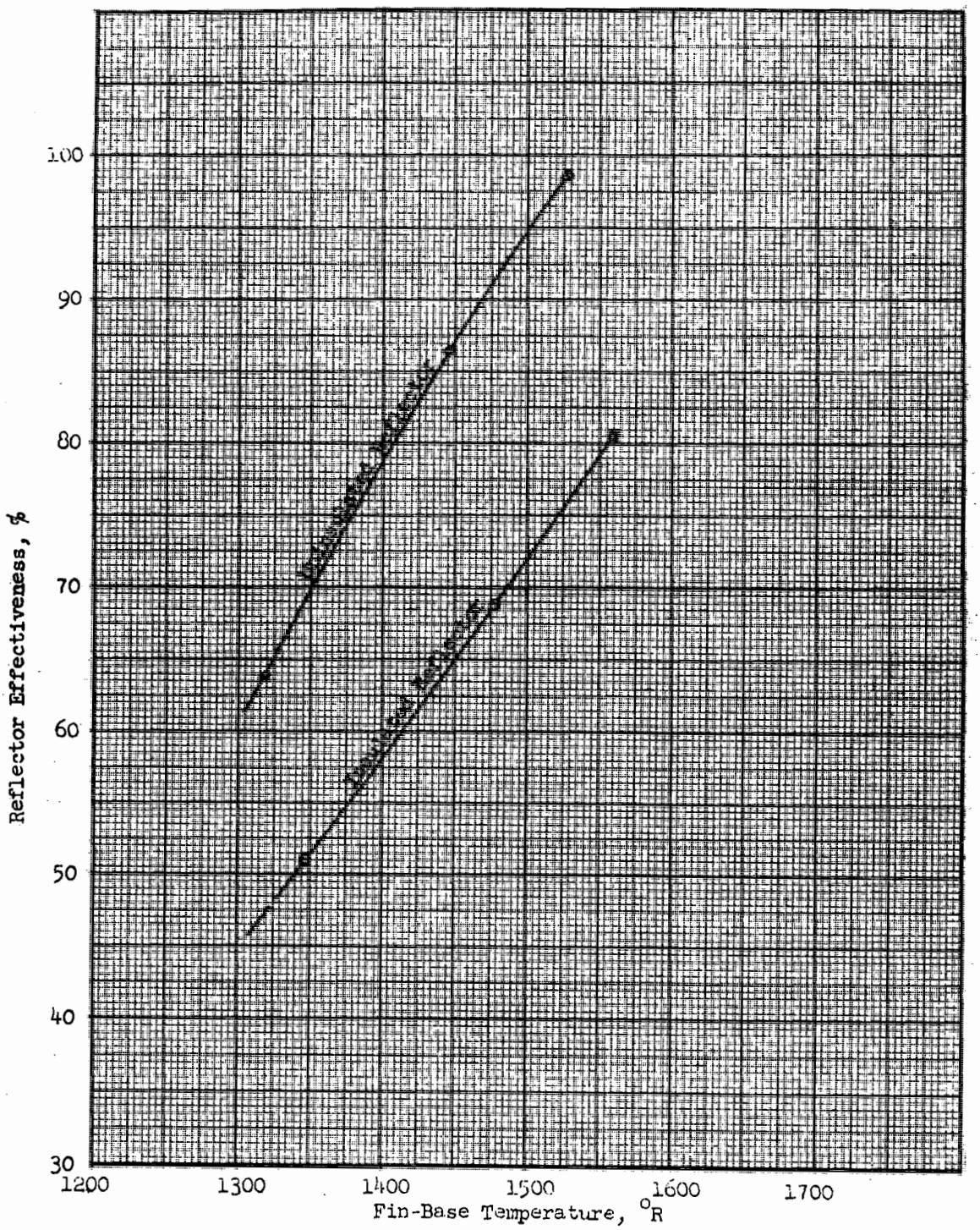

Fig. 17. Reflector Effectiveness vs Fin-Base Temperature with Shutter Open in a Vacuum.

back of the reflector. The effectiveness was 73.5% for the insulated reflector and 96% for the uninsulated reflector at 1510°R.

Other reflector materials, such as gold, should be investigated to determine if higher values of reflectivity and effectiveness for this reflector geometry can be attained.

Heat-Transfer Rate for Uniform Tube Temperature

The heat transfer rates calculated for the ideal case of uniform tube temperature are shown in Fig. 18 for the five surfaces on the radiator as functions of the tube surface temperature for the case of the uninsulated reflector with the shutter open in a vacuum. The heat transfer rate increases at a faster rate with temperature for the back surfaces than the front surfaces because of the temperature dependence of the reflector effectiveness which influences the back side of the radiator and not the front side.

The heat transfer rates calculated for uniform tube temperature for the case of the insulated reflector are shown in Fig. 19. The heat transfer rate for the back surfaces increases with temperature faster than that for the front surfaces in much the same manner as for the case of the uninsulated reflector because of the influence of the reflector effectiveness.

The total calculated heat rating for the radiator tube for both the insulated and uninsulated reflector in a vacuum at a uniform tube temperature is shown in Fig. 20. The design heat load of 4265 Btu/hr-ft was calculated for a temperature of 1538°R for the uninsulated reflector and 1573°R for the insulated reflector. In both cases this is 28°F hotter than the measured average fin-base temperature from Fig. 10. Thus there is only a small difference between the performance as calculated for a uniform tube temperature and that measured for uniform electrical heat generation. This is because only a small part of the heat is radiated from the tube surface proper and a large change in tube-wall temperature between the fins has only a small effect on the overall performance. Most of the difference can be accounted for by the higher temperature at the base of the rear fin for the uniform heat generation case.

ORNL DWG. 67-3177

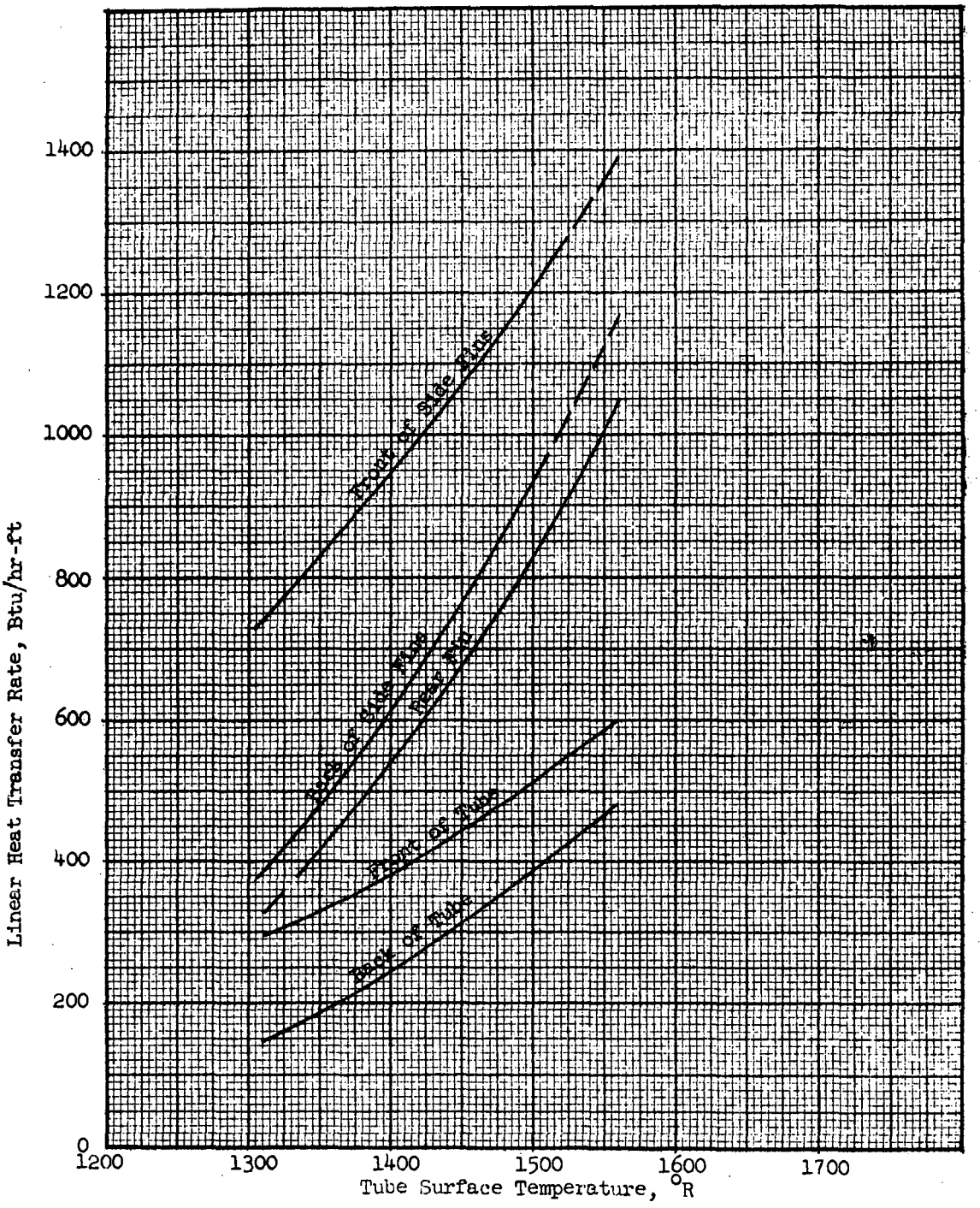

Fig. 18. Calculated Linear Heat Transfer Rate vs Tube Surface Temperature for Each of the Five Portions of the Finned Tube Surface for the Ideal Case in Which the Tube Surface Temperature Is Uniform Around the Perimeter, the Shutter Open, and the Reflector Uninsulated in a Vacuum.

ORNL DWG. 67-3178

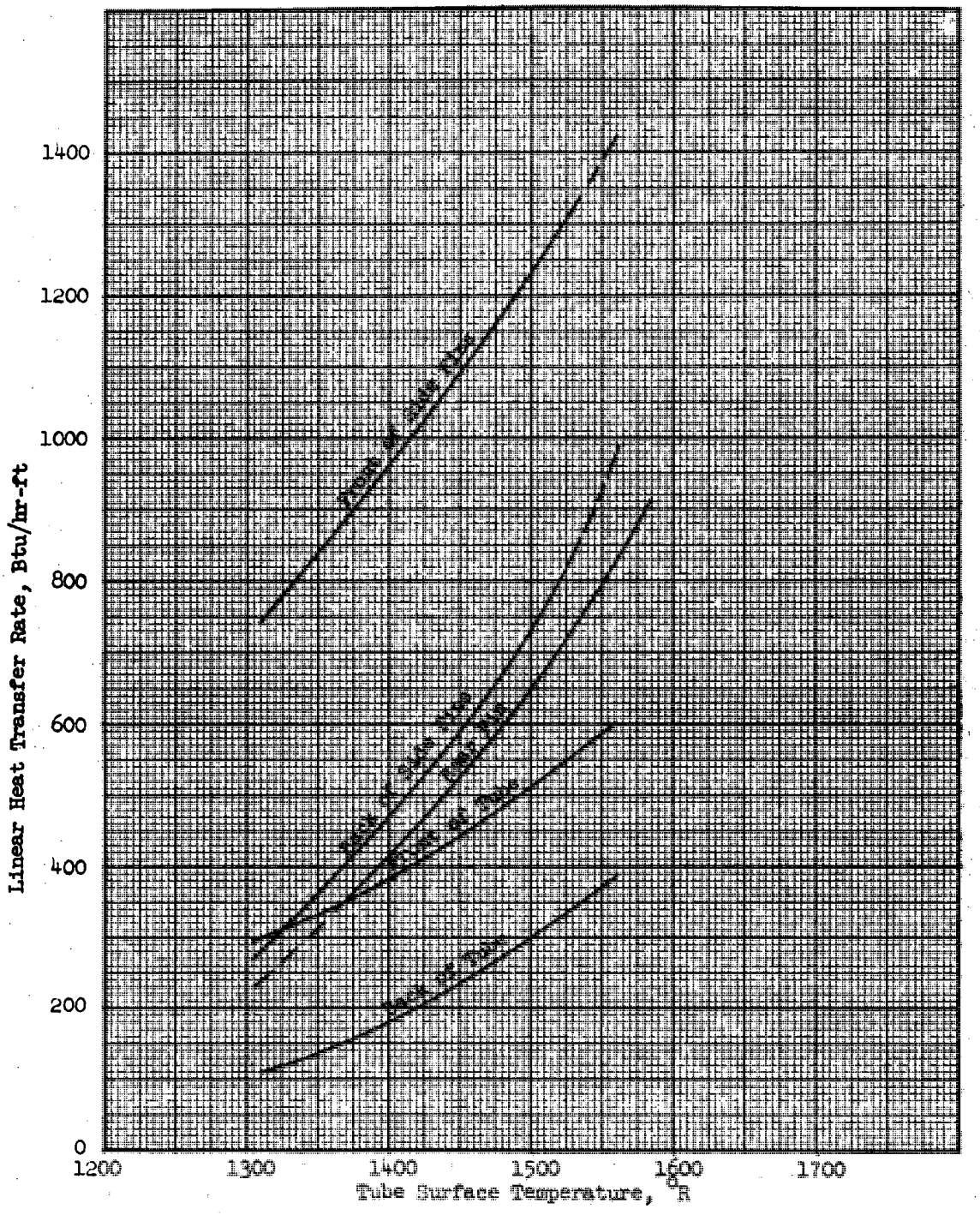

Fig. 19. Calculated Linear Heat Transfer Rate vs Tube Surface Temperature of Each of the Five Portions of the Finned Tube Surface for the Ideal Case in Which the Tube Surface Temperature Is Uniform Around the Perimeter, the Shutter Open, and the Reflector Insulated in a Vacuum.

ORNL DWG. 67-3179

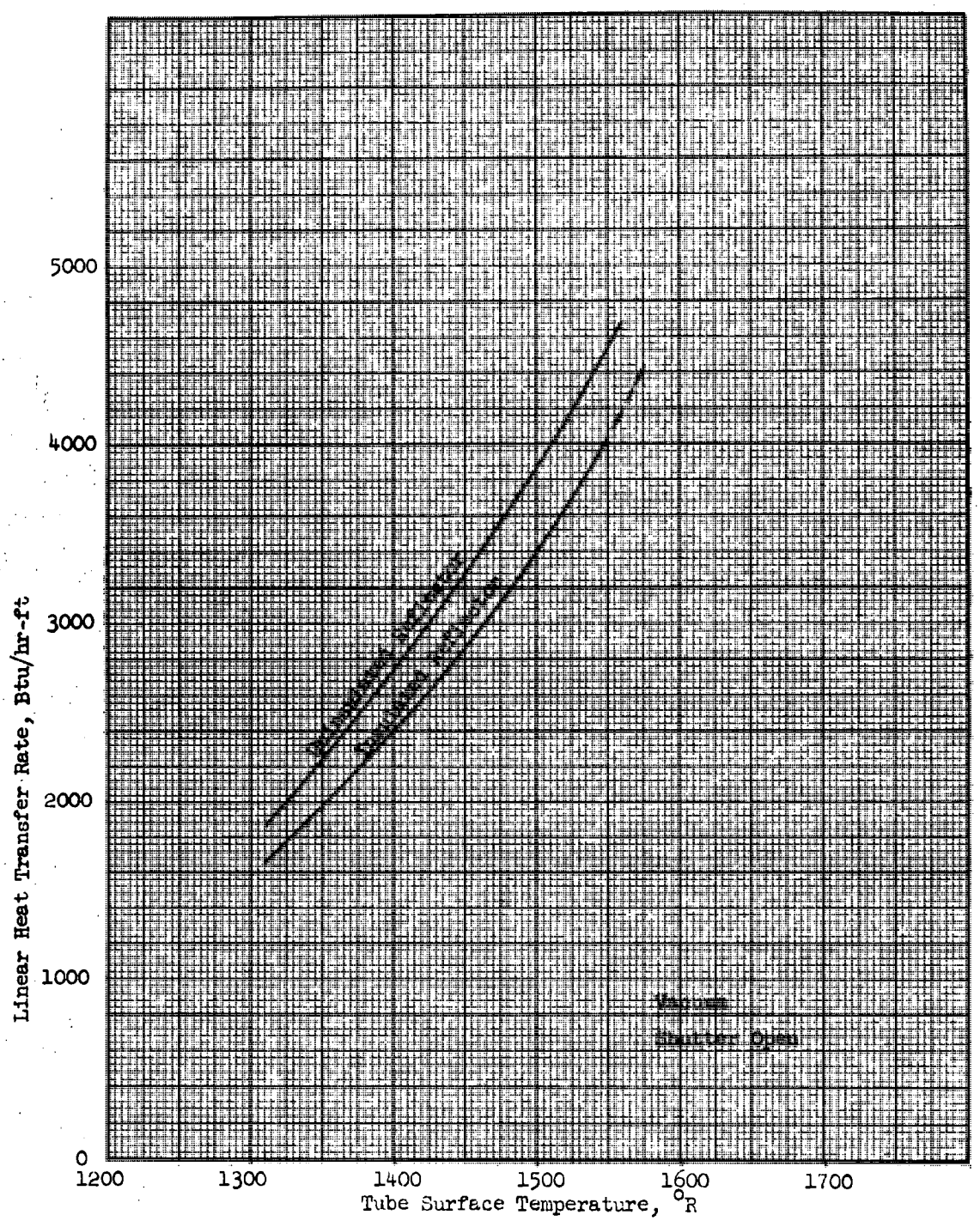

Fig. 20. Calculated Linear Heat Transfer Rate vs Tube Surface Temperature for the Ideal Case in Which the Tube Surface Temperature Is Uniform Around the Perimeter.

SUMMARY OF RESULTS

The results of experiments to obtain the thermal performance of a finned radiator tube with a reflector and a shutter at atmospheric pressure and in a vacuum can be summarized as follows:

1. The LPS design heat load of 4265 Btu/hr-ft was achieved for an average fin-base temperature of 1425°R at atmospheric pressure and 1510°R in a vacuum.

2. The heat transfer rate was reduced with the closed shutter to 2300 Btu/hr-ft at atmospheric pressure and 1700 Btu/hr-ft in a vacuum with the fin-base temperature maintained at the full-load value.

3. The following relationship was found between the linear heat transfer rate and the average fin-base temperature in a vacuum:

$$q = 2.528 \times 10^{-11} T^{5.5}$$

4. The average reflector temperature at the hot end was 795°R at atmospheric pressure, and 860°R in a vacuum at the design heat load.

5. The reflector effectiveness in a vacuum varied from 64% to 98% over a range of temperature from 1320 to 1520°R.

6. The tube surface temperature at the design heat load in a vacuum was calculated to be 1538°R for the ideal case in which the temperature is uniform around the tube.

REFERENCES

1. G. Samuels, M. E. Lackey, and J. J. Tudor, Electrically Heated Mockup, pp. 51-56, Medium-Power Reactor Experiment Quart. Progr. Rept. Dec. 31, 1964, USAEC Report ORNL-3774, Oak Ridge National Laboratory.

2. M. E. Lackey and G. Samuels, Radiator Design, pp. 12-16, Space Power Program Semiann. Progr. Rept. June 30, 1964, USAEC Report ORNL-3683, Oak Ridge National Laboratory.

3. A. P. Fraas, Design and Development Tests of Direct-Condensing Potassium Radiators, pp. 716-736, AIAA Specialists Conference on Rankine Space Power Systems, Vol. I, USAEC Report CONF-651026, October 1965.

4. A. P. Fraas and J. W. Michel, Comparison of 1-, 2-, and 3-Loop Systems for Nuclear Turbine-Generator Space Power Plants of 300 Kw to 5 Mw of Electrical Output, pp. 107-111, USAEC Report ORNL-TM-1366, Oak Ridge National Laboratory.

5. M. Jakob, Heat Transfer, Vol. II, pp. 9-34, John Wiley & Sons, Inc., 1957.

6. A. L. Sopp, Jr. and J. L. Brandt, Reflectivity and Emissivity of Bare and Coated Aluminum, Aluminum Company of America Finishes Division Report 6-62-7, February 1963.

APPENDIXES

APPENDIX A

METHOD OF CALCULATION OF ANGLE FACTORS

Tube Angle Factors

The angle factor for radiant heat transfer from a point on the tube to the heat sink, assuming a tube of infinite length and a cosine distribution of radiation emitted from the surface, can be calculated by the following relation:

$$F_T = \frac{1}{2}(\sin\theta + \sin\phi) \quad , \tag{A.1}$$

where the angles δ and ϕ are the angles defined by Fig. A.1.[5]

The angle factors on the back side of the tube were calculated from Eq. (A.1) at points around the tube at the peripheral angle, β, ranging from 0 to 45°. The angle factors repeated every 45°.

The angle ϕ had a constant value of 90° on the front side of the tube, since a point on the tube had a viewing angle to the left to a tangent line to the surface. For the front side of the tube Eq. (A.1) can be written

$$F_{TF} = \frac{\sin\theta}{2} + \frac{\sin 90°}{2} \quad ,$$

or

$$F_{TF} = \frac{\sin\theta}{2} + \frac{1}{2} \quad . \tag{A.2}$$

The angle factors calculated for both sides of the tube are shown as a function of tube peripheral angle in Fig. A.2. The peripheral angle is the angle β for the back side of the tube and the angle α for the front side.

ORNL DWG. 67-3180

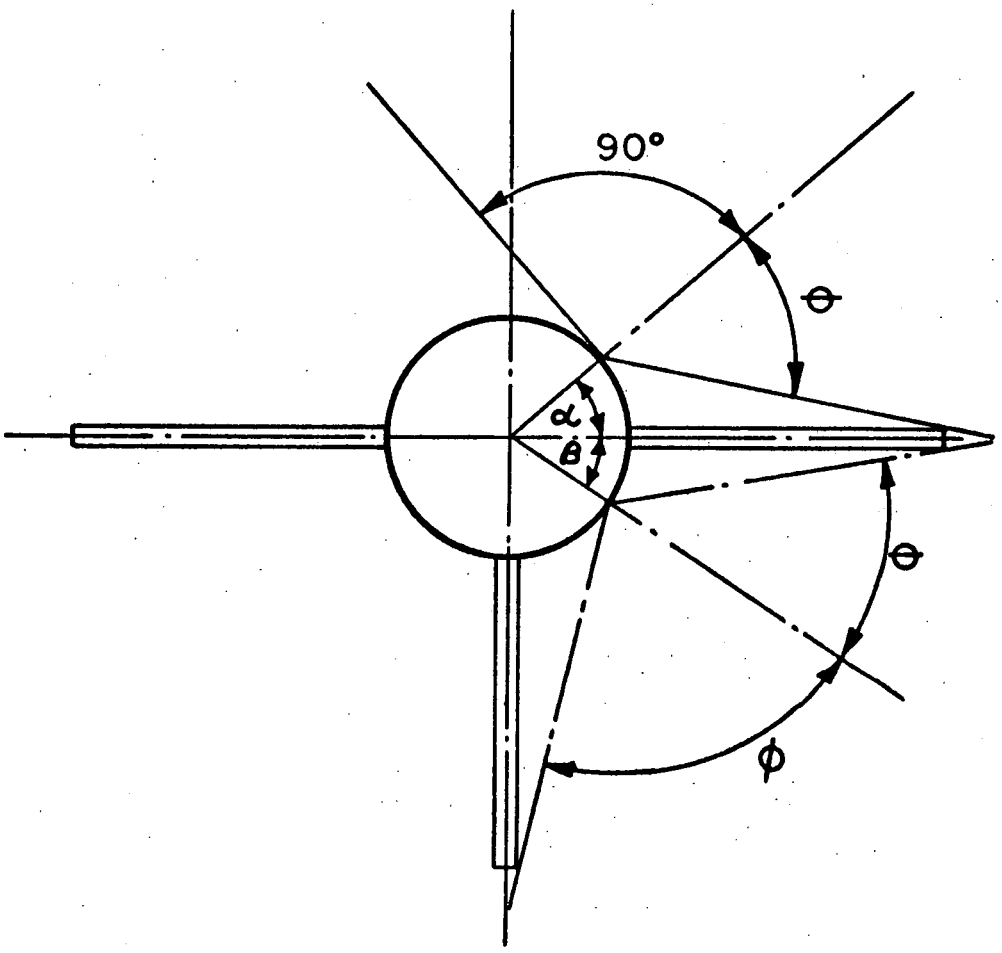

Fig. A.1. Sketch Showing Location of Angles Used to Calculate Local Angle Factors Around Tube.

ORNL DWG. 67-3181

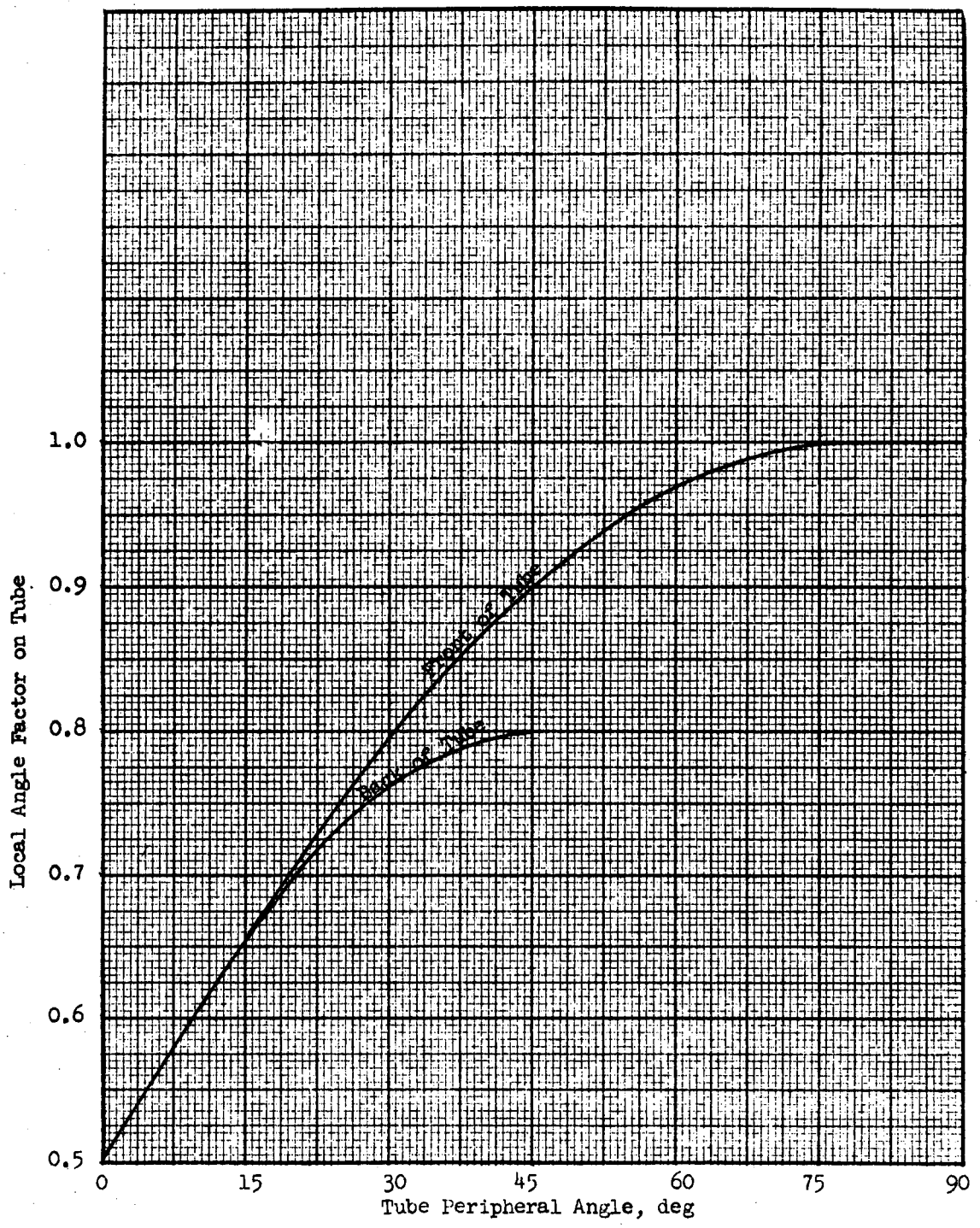

Fig. A.2. Local Angle Factor on Tube vs Tube Peripheral Angle.

Fin Angle Factors

The angle factor for radiation from a point on the fin to the heat sink was calculated by first computing the angle factor from the point on the fin to the tube or adjacent fin and subtracting this from 1. The local angle factor from a point on the fin to the tube or adjacent fin was found by first calculating the angle factor for the fin as a function of distance from the base. This angle factor was calculated as for a system of two rectangular surfaces perpendicular to each other having a common edge by Eq. (31-53), Ref. 5, which is as follows:

$$F_n = \frac{1}{\pi B}\left\{\frac{1}{4}\ln\left[(1+B^2+C^2)^{1+B^2+C^2}(1+B^2)^{1-B^2}(1+C^2)^{1-C^2}(B^2)^{B^2}(C^2)^{C^2}\right]\right.$$

$$-\frac{1}{4}\ln(B^2+C^2)^{B^2+C^2} + B\cdot\mathrm{Tan}^{-1}\frac{1}{B} + C\cdot\mathrm{Tan}^{-1}\frac{1}{C}$$

$$\left.-\sqrt{B^2+C^2}\,\mathrm{Tan}^{-1}\frac{1}{B^2+C^2}\right\} \quad , \qquad (A.3)$$

where

$B = \frac{b}{a}$ = ratio of the variable fin height to the fin length.

$C = \frac{c}{a}$ = ratio of the total height of the adjacent fin to the fin length.

a = fin length = 21 in.

c = fin total height = 1.6 in. for adjacent fin and 0.3125 for tube.

The angle factor over the fin, F_n, was calculated by varying B for different constant values of C, using the IBM 7090 computer. For the angle factor from the front of the side fin to the tube, the value of C was 0.01486. For the angle factor from the back of the side fin to the rear fin, the value of C was 0.07619.

The local angle factor from the fin to the tube or adjacent fin, F_i, was then calculated by dividing the fin into segments and assuming that the angle factor F_n times the area from 0 to n is equal to the sum of the local angle factors times the area of each, which is expressed as

$$F_n A_n = (\Sigma F_i A_i)_{0 \text{ to } n} \tag{A.4}$$

To find any particular value of F_i, we then only have to take the difference between $F_n A_n$ and $F_{n-1} A_{n-1}$ and divide by the area of the local segment A_i, or

$$F_i = \frac{F_n A_n - F_{n-1} A_{n-1}}{A_i} \tag{A.5}$$

This then gives the local angle factor from a point on the fin to the tube or adjacent fin. To find the angle factor from a point on the fin to the heat sink, the local value of F_i is subtracted from 1, or

$$F_F = 1 - F_i \tag{A.6}$$

The local value of the angle factor from the fin to the heat sink for the front and back of the side fin is shown as a function of distance along the fin in Fig. A.3. The angle factors for the rear fin are the same as those for the back of the side fin.

ORNL DWG. 67-3182

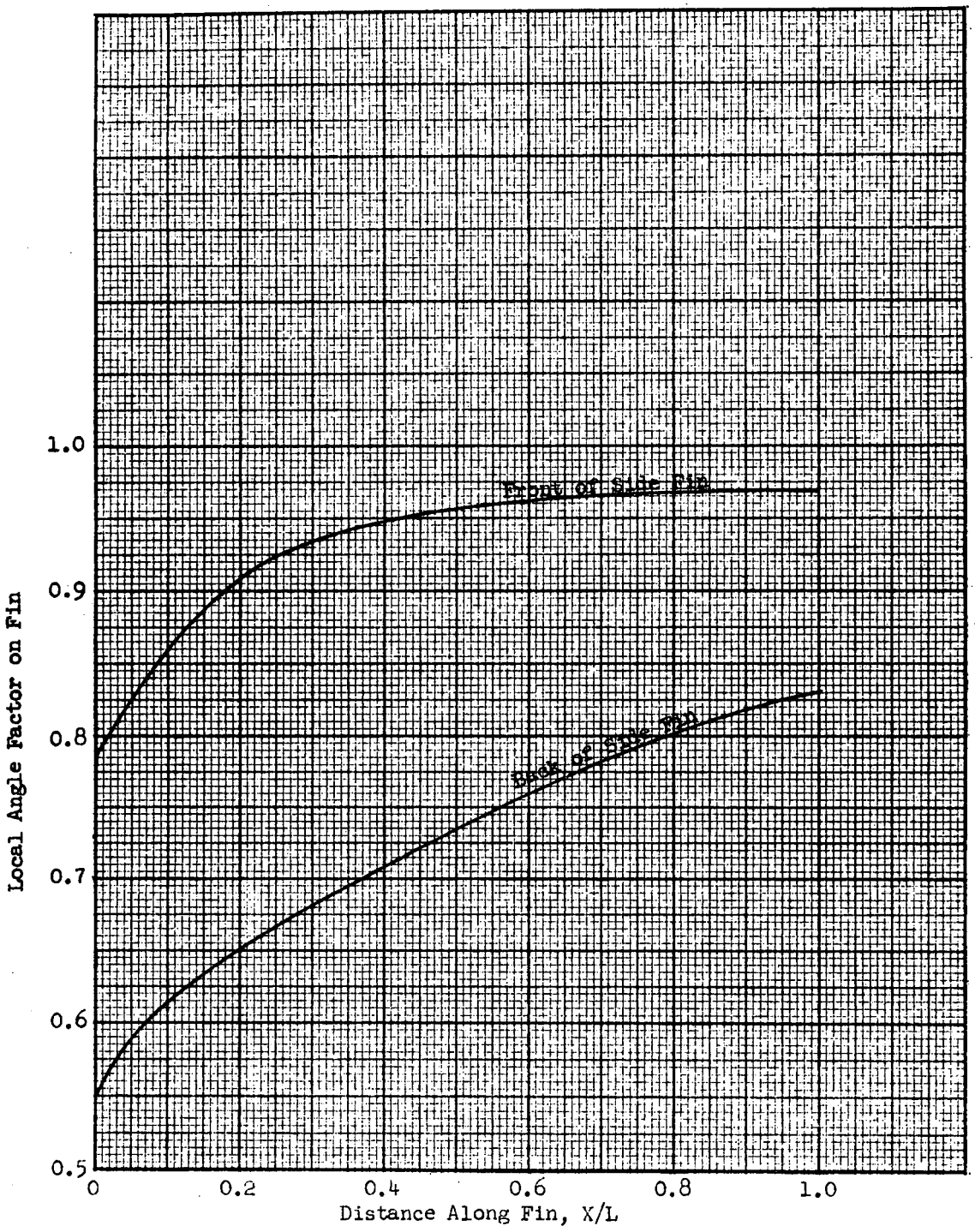

Fig. A.3. Local Angle Factor on Fin vs Distance Along Fin.

APPENDIX B

TABULAR RESULTS OF EXPERIMENTS

The results of the experiments are presented in tabular form on the following pages. The following information is listed for each of the experimental runs: reflector configuration, shutter position, power, air pressure, and surface temperature measured at the location indicated by the thermocouple number. The location of the thermocouples by number is shown in Figs. 5 and 6. A summary of the location of the thermocouples by number is as follows:

Nos. 1 - 13	Radiator surfaces	Upper location
Nos. 14 - 26	Radiator surfaces	Lower location
Nos. 27 - 30	Reflector surface	Upper location
Nos. 31 - 34	Reflector surface	Lower location
Nos. 35 - 37	Water-wall surface	Opposite reflector, upper location
Nos. 38 - 40	Water-wall surface	Opposite reflector, lower location
Nos. 41 - 43	Water-wall surface	Opposite radiator, upper location
Nos. 44 - 46	Water-wall surface	Opposite radiator, lower location
Nos. 47 - 49	Shutter surface	Upper location
Nos. 50 - 52	Shutter surface	Lower location

Table B.1. Tabular Results of Experiments

Run Numbers	1	2	3	4	5	6	7	8	9
Reflector: Uninsulated									
Shutter: Open									
Pressure (mm Hg abs)	750.57	749.43	736.6	749.05	2.4	2.1	2.2	2.5	2.0
Power (watts)	4312	3200	1980	946	4301	3270	1974	950	597
Thermocouple No.	Temperature (°F)								
1	856	792	695	553	932	874	776	646	566
2	889	820	716	566	962	899	794	657	575
3	979	894	772	602	1050	972	848	692	601
4	1055	962	823	635	1124	1036	897	723	624
5	1017	928	798	619	1089	1006	873	706	613
6	897	826	722	570	972	905	798	658	577
7	—	—	—	—	—	—	—	—	—
8	1064	968	828	638	1136	1045	903	728	628
9	967	883	762	595	1038	961	839	685	596
10	887	816	713	564	961	896	793	656	575
11	846	780	686	547	921	863	768	640	563
12	1135	1026	872	664	1207	1107	952	760	651
13	1149	1039	881	670	1221	1123	962	767	656
14	808	752	662	529	885	831	739	613	540
15	840	780	684	543	913	857	757	624	549
16	929	854	742	579	1001	931	812	661	576
17	1080	988	847	652	1158	1068	923	742	639
18	996	915	790	617	1073	993	866	703	611
19	900	834	720	578	977	912	805	664	582
20	860	801	704	561	939	877	779	646	569
21	1060	973	833	645	1141	1048	907	731	631
22	998	918	791	618	1079	995	865	704	611
23	890	827	722	575	969	901	796	659	578
24	850	793	696	558	935	873	770	645	568
25	1152	1053	893	683	1226	1127	966	774	662
26	1167	1065	900	687	1247	1146	980	782	667

Table B.1. (continued)

Run Numbers	1	2	3	4	5	6	7	8	9
Reflector: Uninsulated									
Shutter: Open									
Pressure (mm Hg abs)	750.57	749.43	736.6	749.05	2.4	2.1	2.2	2.5	2.0
Power (watts)	4312	3200	1980	946	4301	3270	1974	950	597
Thermocouple No.	Temperature (°F)								
27	329	301	265	204	391	370	325	268	232
28	345	315	279	212	411	389	343	282	244
29	348	317	280	213	411	389	344	282	245
30	334	305	269	207	396	374	329	271	235
31	279	255	225	172	384	363	320	263	229
32	297	270	239	181	403	382	338	277	241
33	297	271	240	182	403	381	338	278	241
34	286	261	231	176	392	370	327	268	234
35					63	58	61	62	
36					63	58	61	62	
37					61	56	60	61	
38					58	54	58	59	
39					58	54	58	59	
40					57	54	57	59	
41					69	60	62	61	
42					72	63	63	62	
43					72	64	64	62	
44						—	—	—	
45					66	58	60	59	
46					67	59	61	60	

Table B.1. (continued)

Run Numbers	10	11	12	13	14	15	16	17	18
Reflector: Uninsulated									
Shutter: Closed									
Pressure (mm Hg abs)	741.43	736.35	736.35	735.58	741.43	2.2	1.9	2.1	2.5
Power (watts)	2149	1688	1119	586	235.6	1653	1252	790	280.5
Thermocouple No.	Temperature (°F)								
1	898	826	719	565	380	986	921	809	584
2	921	846	734	575	384	1001	934	819	588
3	979	896	773	602	399	1050	974	849	603
4	1019	930	802	622	410	1077	998	868	613
5	990	905	782	608	403	1054	978	852	604
6	906	832	810	569	382	985	918	806	580
8	1025	935	806	623	411	1085	1005	873	615
9	977	893	772	600	398	1048	974	849	602
10	928	851	740	578	386	1011	942	826	635
11	901	827	721	566	380	989	923	812	584
12	1085	988	847	649	423	1145	1058	914	635
13	1094	995	853	653	425	1152	1065	918	638
14	847	779	679	533	361	960	897	788	569
15	870	799	694	544	367	976	953	799	574
16	924	888	733	570	380	1019	948	827	589
17	1017	929	802	620	409	1103	1022	887	623
18	954	871	758	591	394	1047	972	848	603
19	887	817	713	561	379	991	924	811	584
20	858	791	693	548	372	967	902	795	576
21	1006	920	795	616	407	1094	1011	878	619
22	978	895	775	602	399	1074	995	866	613
23	908	836	729	571	383	1017	946	829	594
24	882	813	711	559	377	1001	933	819	589
25	1079	983	846	647	423	1167	1077	928	644
26	1087	990	851	650	423	1176	1084	934	645
27	407	370	315	239	160	504	467	406	289

Table B.1. (continued)

Run Numbers	10	11	12	13	14	15	16	17	18
Reflector: Uninsulated									
Shutter: Closed									
Pressure (mm Hg abs)	741.43	736.35	736.35	735.58	741.43	2.2	1.9	2.1	2.5
Power (watts)	2149	1688	1119	586	235.6	1653	1252	790	280.5
Thermocouple No.	Temperature (°F)								
28	412	375	320	243	163	506	470	410	293
29	417	378	323	245	164	507	471	410	293
30	411	372	318	241	161	500	464	405	288
31	338	306	258	196	178	491	456	397	282
32	345	313	265	201	137	496	461	403	287
33	346	313	265	201	137	495	461	404	288
34	339	306	259	196	135	492	458	400	284
47	388	343	282	207	140	595	539	448	284
49	386	341	282	208	141	584	530	440	280
50	274	241	198	147	104	595	539	444	276
51	269	237	194	144	102	594	539	444	276
52	269	237	195	145	103	589	535	442	276

Table B.1. (continued)

Run Numbers	19	20	21	22	23	24	25	26	27
Reflector: Uninsulated									
Shutter: Closed (flat shutter)									
Pressure (mm Hg abs)	737.36	737.11	735.08	736.6	736.6	1.9	2.0	2.8	2.6
Power (watts)	1530	1186	802	447	188.3	1451	1143	759	297
Thermocouple No.	Temperature (°F)								
1	918	843	731	574	384	996	927	811	582
2	934	856	741	581	387	1009	940	820	587
3	980	896	772	602	398	1052	975	848	602
4	1008	921	750	617	406	1078	999	867	613
5	984	900	776	606	401	1047	980	853	605
6	915	840	728	573	384	992	924	809	582
8	1014	927	796	620	408	1087	1006	873	615
9	980	896	771	602	398	1055	977	849	602
10	944	866	748	586	389	1021	948	827	590
11	923	848	733	576	385	1000	930	813	583
12	999	950	819	630	411	1089	991	899	630
13	1070	976	835	644	419	1143	1054	910	635
14	800	735	632	483	317	971	903	788	565
15	819	753	646	493	322	987	916	798	570
16	864	791	677	514	334	1026	952	826	586
17	940	860	734	513	358	1103	1021	884	621
18	888	814	698	533	346	1048	973	846	602
19	834	766	661	508	334	996	948	812	582
20	812	747	645	497	329	973	908	796	575
21	936	853	729	553	356	1091	1011	876	617
22	914	832	711	538	347	1031	996	862	608
23	860	784	673	512	334	1021	949	827	589
24	834	760	653	498	325	1005	936	817	584
25	983	890	755	563	356	–	–	–	632
26	1006	909	774	579	368	1167	1078	924	639
27	424	387	332	255	171	498	464	398	280

Table B.1 (continued)

Run Numbers	19	20	21	22	23	24	25	26	27
Reflector: Uninsulated									
Shutter: Closed (flat shutter)									
Pressure (mm Hg abs)	737.36	737.11	735.08	736.6	736.6	1.9	2.0	2.8	2.6
Power (watts)	1530	1186	802	447	188.3	1451	1143	759	297
Thermocouple No.	Temperature (°F)								
28	433	395	338	259	174	507	471	407	287
29	437	398	340	260	175	509	443	409	289
30	433	394	336	258	173	501	466	402	284
31	324	291	243	180	122	490	454	394	278
32	338	303	252	187	126	501	464	403	285
33	340	304	253	188	126	501	465	404	286
34	331	295	246	183	123	496	460	400	283
48	563	495	411	310	202	678	606	511	346
49	495	445	375	286	188	597	547	467	320
50	384	338	277	201	131	595	546	466	319
51	443	388	315	224	142	654	597	506	339
52	413	363	297	213	138	624	575	490	332

Table B.1. (continued)

Run Numbers	28	29	30	31	32	33	34
Reflector: Insulated							
Shutter: Open							
Pressure (mm Hg abs)	729.36	733.67	734.06	734.06	2.5	3.1	2.4
Power (watts)	4279	3205	1972	936	4242	3200	1961
Thermocouple No.	Temperature (°F)						
1	873	812	708	567	955	895	796
2	907	841	730	580	987	923	816
3	999	918	788	618	1076	997	871
4	1076	986	840	652	1156	1067	924
5	1041	955	817	637	1125	1040	903
6	922	853	741	587	1011	944	831
8	1087	995	847	656	1171	1080	933
9	995	915	785	615	1076	997	870
10	916	849	736	584	1001	934	824
11	877	815	711	568	962	901	799
12	1148	1048	885	680	1231	1132	974
13	1164	1062	896	687	1245	1144	984
14	815	759	663	533	911	854	760
15	850	788	685	547	942	880	779
16	938	862	742	583	1031	956	836
17	1093	1000	850	659	1195	1104	955
18	1009	927	794	623	1115	1034	901
19	916	848	736	585	1022	955	843
20	873	812	708	567	984	923	818
21	1082	990	843	654	1177	1090	943
22	1022	938	802	628	1121	1040	904
23	917	849	736	586	1013	947	836
24	877	815	710	569	980	920	815
26	1178	1031	904	693	1277	1179	1012
27	443	402	336	257	583	551	476
28	456	414	347	266	607	572	495

Table B.1. (continued)

Run Numbers	28	29	30	31	32	33	34
Reflector: Insulated							
Shutter: Open							
Pressure (mm Hg abs)	729.36	733.67	734.06	734.06	2.5	3.1	2.4
Power (watts)	4279	3205	1972	936	4242	3200	1961
Thermocouple No.	Temperature (°F)						
29	462	419	350	268	612	576	499
30	456	413	345	264	600	564	487
31	341	308	257	198	587	553	480
32	357	323	269	206	609	573	498
33	370	335	279	212	615	577	
34	372	337	280	213	606	569	

INTERNAL DISTRIBUTION

1. G. M. Adamson, Jr.
2. S. J. Ball
3. S. E. Beall
4. H. C. Claiborne
5. F. L. Culler, Jr
6. J. E. Cunningham
7. J. H. DeVan
8. E. P. Epler
9. J. Foster
10-29. A. P. Fraas
30. A. G. Grindell
31. W. O. Harms
32. P. N. Haubenreich
33. R. S. Holcomb
34. S. I. Kaplan
35. P. R. Kasten
36. T. W. Kerlin
37. M. E. Lackey
38. M. E. LaVerne
39. M. I. Lundin
40. F. E. Lynch
41. R. N. Lyon
42. H. G. MacPherson
43. R. E. MacPherson
44. H. C. McCurdy
45. J. W. Michel
46. A. J. Miller
47. A. M. Perry
48. G. Samuels
49. A. W. Savolainen
50. J. L. Scott
51. O. L. Smith
52. I. Spiewak
53. D. B. Trauger
54. A. M. Weinberg
55. J. R. Weir, Jr.
56. G. D. Whitman
57. J. V. Wilson
58. M. M. Yarosh
59. Gale Young
60-61. Central Research Library
62-63. Y-12 Document Reference Section
64-66. Laboratory Records
67. Laboratory Records — Record Copy
68. ORNL Patent Office

EXTERNAL DISTRIBUTION

69. C. H. Armbruster, Wright Air Development Center, Dayton, Ohio
70. G. K. Dicker, AEC, Washington
71-80. H. B. Finger, AEC, Washington
81. Graham Hagey, NASA, Houston
82. Carl E. Johnson, AEC, Washington
83. J. D. Lafleur, AEC, Washington
84. S. Lieblein, NASA, Cleveland, Ohio
85-89. Bernard Lubarsky, NASA, Cleveland, Ohio
90. James Lynch, NASA, Washington, D. C.
91. T. W. McIntosh, AEC, Washington, D. C.
92. Don Packey, NASA, Cleveland, Ohio
93. Benjamin Pinkel, Rand Corp., Santa Monica, California
94. Fred Schulman, NASA, Washington
95. Abe Silverstein, NASA, Cleveland, Ohio
96. Jack Stearns, JPL, Pasadena, California
97. H. J. Stewart, JPL, Pasadena, California
98. G. C. Szego, IDA, Arlington, Va.
99. Gordon Woodcock, Nasa, Huntsville, Ala.
100-114. Division of Technical Information Extension (DTIE)
115. Research and Development Division, ORO
116-117. Reactor Division, ORO